MLL2_Ex31_PCR_R3*	GCAGCTGTTTCCTTCTCCTG	60.1			
MLL2_Ex31_Seq_F1	GCAGGACCCCTTTGGACT	60.1			
MLL2_Ex31_Seq_R1	CAGGTGGGGTAGTGTGGAAT	59.7			
MLL2_Ex31_Seq_F2	CTCGGGCATCTCAGGTAGAG	60.0			
MLL2_Ex31_Seq_R2	GAGCACAGCAGCTCTCAGG	63.2			
MLL2_Ex31_Seq_F3	TTCACTTTCCCTCAGGCAGT	59.8			
MLL2_Ex31_Seq_R3	GTTTGTGCTTTGAGGCTTGC	61.0			
MLL2_Ex32_33_PCR_F1	CCCCCTATATCGCTCCTGTC	60.8	Exons 32 and 33	620	0.5
MLL2_Ex32_33_PCR_R1	GCAGTGAGGGAGAAAAGGAA	59.4			
MLL2_Ex34_PCR_F2	TCCTTCCTCACTGCCCTAAG	59.4	Exon 34	2019	2.0
MLL2_Ex34_PCR_R2	TCTAGCCTCAGTGCCCATTT	59.8			
MLL2_Ex34_Seq_F1	TCAGAGACCCCGTTTTTCAC	60.1			
MLL2_Ex34_Seq_R1	GTGGGGTGTTGGATGAAGAC	60.5			
MLL2_Ex34_Seq_F2	GAGACCAATGACCCCCACTT	61.2			
MLL2_Ex34_Seq_R2	CAAGGGTCCTGGCTCCAC	61.7			
MLL2_Ex34_Seq_F3	TGCTCATTGAGGACCTGTTG	59.8			
MLL2_Ex34_Seq_R3	CTCATGTGGCAAAGACATGG	60.1			
MLL2_Ex35_38_PCR_F1	GCACGGTGCAAGTAAAAACA	59.8	Exons 35 to 38	1167	1.5
MLL2_Ex35_38_PCR_R1	AGGGTCGGAGAGGTCAGG	60.2			
MLL2_Ex35_38_Seq_F1	GTGGTCAGGTGGGAGTAGGA	60.0			
MLL2_Ex35_38_Seq_R1	TGCAATGAGAGAGGCTGCTA	59.9			
MLL2_Ex39_PCR_F2	ACTTCAGCCTAGCACCCAGA	60.0	Exon 39 - first half	1585	1.5
MLL2_Ex39_PCR_R2	TTGGACAAGCAGGAGTTGTG	59.9			
MLL2_Ex39_Seq_F2	CTTCTTCCCTGGCAACCTT	59.3			
MLL2_Ex39_Seq_R2	GGATTGCCACCTGTCCTAGA	60.1			
MLL2_Ex39_Seq_F3	GGACACAGGCTGGTCACAG				
MLL2_Ex39_Seq_R3	GCTGCTGAAGCTGCTGTAAA				
MLL2_Ex39_PCR_F3	TAGACCCAGCCGTTTCTTCA	60.8	Exon 39 - second half	1521	1.5
MLL2_Ex39_PCR_R3	ACCCAGGCTCACTCATTCTG	60.3			
MLL2_Ex39_Seq_F4	TTAAGTCCTCAGCAGCAGCA	59.9			
MLL2_Ex39_Seq_R4	TGTCTGTGGTCCAGGGAAG	59.6			
MLL2_Ex39_Seq_F5	CAGAAACCCAGAAGCCAGAG	60.0			
MLL2_Ex39_Seq_R5	GCCTCCCTCTTCACTGACTG	60.0			
MLL2_Ex40_42_PCR_F1	AGCCTGGGTCAGACAGAAGA	60.0	Exons 40 to 42	960	1.0
MLL2_Ex40_42_PCR_R1	ACCTCAGGTGCCCTGTTATG	60.0			
MLL2_Ex40_42_Seq_F1	GAAGTTCTTGGGAAGGTGAGG	60.1			
MLL2_Ex40_42_Seq_R1	GCAAGATGGCATAGGGAGAC	59.7			
MLL2_Ex43_45_PCR_F1	CAAACTGGTAGGTGGGAGGA	60.0	Exons 43 to 45	919	1.0
MLL2_Ex43_45_PCR_R1	TCTAGCCCAGGCTTTCACAT	59.8			
MLL2_Ex43_45_Seq_F1	GAAATGGGGATGAGGAACAA	59.7			
MLL2_Ex43_45_Seq_R1	CAGACTCCCCTCCCAAATCT	60.5			
MLL2_Ex46_47_PCR_F1	CCCACCCAGCTGGTAGTAGA	60.1	Exons 46 and 47	510	0.5
MLL2_Ex46_47_PCR_R1	CTCCCAAAGCACTGGGATTA	60.1			
MLL2_Ex48_PCR_F2	GAGGCTGTCTAGGGCAAAGA	59.6	Exon 48	1375	1.5
MLL2_Ex48_PCR_R2	GGGAAGGAGGATCATTCACA	59.9			
MLL2_Ex48_Seq_F2	TTCTGTCATGAGGAGGGTGA	59.2			
MLL2_Ex48_Seq_R2	CAGGTCCAGGTTCAGCAGAC	60.9			
MLL2_Exon48_Seq_F1	TGCCCCAATGTCTACCATTT	60.2			

MLL2_Exon48_Seq_R1	ACCTCGTCCCGCTCAATGTA	62.9			
MLL2_Ex49_50_PCR_F1	GCAGTTCTGGATTGGGGTTA	59.9	Exons 49 and 50	512	0.5
MLL2_Ex49_50_PCR_R1	GACCAGAGGATCCCTGTCAA	60.1			
MLL2_Ex51_54_PCR_F1	CAGAGGAGGTGGGTGGTATG	60.4	Exons 51 to 54	1253	1.5
MLL2_Ex51_54_PCR_R1	CTGGCTGCTACCTCTCTTCC	59.2			
MLL2_Ex51_54_Seq_F1	CTCCTACCTGATCCCACAGC	59.7			
MLL2_Ex51_54_Seq_R1	GTCAGGGATGTCAGGCAACT	60.1			

Notes:
Primers with 'PCR' in the name were used for amplification.
Primers with 'Seq' in the name were nested sequencing primers for the associated amplicon.
DNA sequencing reactions were performed using all 'PCR' and 'Seq' primers.
*Exon 31 PCR primers require half the amount of $MgCl_2$ listed in "Reaction Conditions".

PCR Components	
Reagent	**1X (µL)**
10X PCR Buffer	2.5
50 mM $MgCl_2$	1.25
1.25 mM dNTPs	2
5M Betaine	5
Forward Primer (1 µM)	5
Reverse Primer (1 µM)	5
H_2O	2
Taq Polymerase (5U/µL)	0.25
DNA Template (10ng/µL)	2
Total	25

PCR Cycling Parameters	
95°C for 5 min	
95°C for 0.5 min Tm°C for 0.5 min 72°C for 0.5-2 min	35 cycles
72°C for 10 min 4°C hold	

Supplementary Table II: List of mutations found in MLL2 by exome and targeted re-sequencing

Kindred	Indiv	Exome Sequenced	Previously Published Mutation Name (Ng, S.B. et al.)	Mutation Name	Exon	Predicted Amino Acid Change	Confirmed as de novo	Positiona	Comments
1	1	yes	c.G15195A	c.15195G>A	48	p.W5065X	+	chr12:47706821	The individuals in kindred 1 are monozygotic twins.
	2	no	c.G15195A	c.15195G>A	48	p.W5065X	+	chr12:47706821	
2		yes	c.C6010T	c.6010C>T	28	p.Q2004X	+	chr12:47722238	
3		yes	c.C12697T	c.12697C>T	39	p.Q4233X	+	chr12:47712058	
4		yes	c.C8488T	c.8488C>T	34	p.R2830X	-	chr12:47718918	
5		yes	--	--	--	--	--	--	
6		yes	c.11794_11797delCAAC	c.11794_11797delCAAC	39	p.Q3932SfsX46	+	chr12:47712958-61	
7		yes	c.T15618G	c.15618T>G	48	p.Y5206X	+	chr12:47706398	
8		yes	c.3585_3586insA	c.3585dupA	11	p.P1196TfsX11	+	chr12:47730053	
9		yes	c.C6295T	c.6295C>T	31	p.R2099X	+	chr12:47721525	
10		yes	c.6595delT	c.6595delT	31	p.Y2199IfsX65	+	chr12:47721225	
11		no	c.G15326T	c.15326G>T	48	p.C5109F	+	chr12:47706690	
12		no	c.G15536A	c.15536G>A	48	p.R5179H	+	chr12:47706480	
13		no	c.C11149T	c.11149C>T	39	p.Q3717X	+	chr12:47713606	
14		no	c.15444_15445delTT	c.15446_15447delTT	48	p.F5149CfsX9	-	chr12:47706569-70	
15		no	c.C15217T	c.15217C>T	48	p.Q5073X	-	chr12:47706799	
16		no	c.C9961T	c.9961C>T	34	p.R3321X	-	chr12:47717445	
17		no	c.C14710T	c.14710C>T	48	p.R4904X	-	chr12:47707306	
18		no	c.5875_5891dup17	c.5877_5893dup17	28	p.E1965GfsX88	-	chr12:47722355-71	
19		no	c.G15536A	c.15536G>A	48	p.R5179H	-	chr12:47706480	
20		no	c.C12703T	c.12703C>T	39	p.Q4235X	-	chr12:47712052	
21		no	c.C12241T	c.12241C>T	39	p.Q4081X	-	chr12:47712514	
22		no	c.C13390T	c.13390C>T	39	p.Q4464X	+	chr12:47711365	
23		no	c.G15641A	c.15641G>A	48	p.R5214H	-	chr12:47706375	
24		no	--	--	--	--	--	--	
25	1	no	c.A13580T	c.13579A>T	40	p.K4527X	*	chr12:47711035	The cDNA position was identified incorrectly as c.13580A>T by Ng, SB et al. [2010]
	2	no	c.A13580T	c.13579A>T	40	p.K4527X	-	chr12:47711035	The cDNA position was identified incorrectly as c.13580A>T by Ng, SB et al. [2010]
26		no	c.C16501T	c.16501C>T	53	p.R5501X	-	chr12:47702113	
27	1	no	--	--	--	--	--	--	
	2	no	--	--	--	--	--	--	
28		no	--	--	--	--	--	--	
29		no	c.C10738T	c.10738C>T	38	p.Q3580X	-	chr12:47714119	
30		no	--	--	--	--	--	--	
31		no	c.C16360T	c.16360C>T	52	p.R5454X	-	chr12:47702382	
32		no	--	--	--	--	--	--	
33		no	--	c.840-1G>A	7	splicing error	-	chr12:47733372	The mutation was identified after publication by Ng, SB et al. [2010]
34		no	--	--	--	--	--	--	
35		no	c.4956_4957insG	c.4958dupG	19	p.E1654X	-	chr12:47724799	
36		no	c.10599_10630del32	c.10599_10630del32	38	p.V3534QfsX11	-	chr12:47714227-58	
37		no	--	--	--	--	--	--	
38		no	c.C13606T	c.13606C>T	40	p.R4536X	-	chr12:47711008	
39		no	c.G16019T	c.16019G>T	50	p.R5340L	-	chr12:47704661	
40		no	c.C4843T	c.4843C>T	19	p.R1615X	-	chr12:47724914	
41		no	c.C16391T	c.16391C>T	52	p.T5464M	-	chr12:47702351	
42		no	--	--	--	--	--	--	
43		no	--	--	--	--	--	--	
44		no	--	--	--	--	--	--	
45		no	c.C16360T	c.16360C>T	52	p.R5454X	-	chr12:47702382	It was determined that this kindred is a duplicate of kindred 31 after publication by Ng, SB et al. [2010]
46		no	--	--	--	--	--	--	
47		no	--	c.4412G>A	15	p.C1471Y	-	chr12:47726665	The mutation was identified after publication by Ng, SB et al. [2010]
48		no	--	--	--	--	--	--	After sequencing MLL2, it was determined by aCGH that this individual is mosaic for trisomy or tetrasomy of chromosome 12.
49		no	--	--	--	--	--	--	After sequencing MLL2, it was determined by aCGH that this individual has Sotos Syndrome.
50		no	c.1324delC	c.1328delC	10	p.P443HfsX487	-	chr12:47732405	The protein position was identified incorrectly as p.P442HfsX487 by Ng, SB et al. [2010]
51		no	--	--	--	--	--	--	After sequencing MLL2, it was determined by aCGH that this individual has a translocation t(8;18)(q22;q21).
52	1	no	c.C16391T	c.16391C>T	52	p.T5464M	*	chr12:47702351	
	2	no	c.C16391T	c.16391C>T	52	p.T5464M	-	chr12:47702351	
53		no	--	--	--	--	--	--	
54		no	N/A	c.15785-1G>C	49	splicing error	+	chr12:47704997	
55		no	N/A	I	I	I	I	I	Two variants were found in this individual [c.15922-2A>C(+)c.15958C>T]. We could not determine which variant is pathogenic.
56		no	N/A	c.5865_5867delTAGinsCCC	27	p.R1956PfsX92	-	chr12:47722611-13	
57		no	N/A	c.13285C>T	39	p.Q4429X	+	chr12:47711470	
58		no	N/A	--	--	--	--	--	
59		no	N/A	c.11047C>T	39	p.Q3683X	-	chr12:47713708	
60		no	N/A	c.7228C>T	31	p.R2410X	-	chr12:47720592	

61		no	N/A	---	---	---	---	---	After sequencing MLL2, it was determnined by aCGH that this individual carries a 977kb deletion on chromosome 19q13.4
62		no	N/A	---	---	---	---	---	
63		no	N/A	c.7650delT	31	p.V2551SfsX32	-	chr12:47720170	
64		no	N/A	c.702delG	6	p.P235QfsX26	-	chr12:47733663	
65		no	N/A	c.16342C>T	52	p.R5448X	-	chr12:47702400	
66		no	N/A	c.16360C>T	52	p.R5454X	-	chr12:47702382	
67		no	N/A	---	---	---	---	---	
68		no	N/A	c.5832C>A	27	p.Y1944X	-	chr12:47722646	
69		no	N/A	c.9831_9833dupGCA	34	p.Q3282dup	-	chr12:47717573-75	
70		no	N/A	c.15073_15080dup8	48	p.D5028YfsX26	-	chr12:47706936-43	
71		no	N/A	c.15142C>T	48	p.R5048C	-	chr12:47706874	
72		no	N/A	c.15641G>A	48	p.R5214H	-	chr12:47706375	
73		no	N/A	---	---	---	---	---	
74		no	N/A	I	I	I	I	I	Two variants were found in this individual [c.10812_10832dup21(+)c.14485dupG]. Variant c.10812_10832dup21 was also found in this patient's unaffected mother.
75		no	N/A	---	---	---	---	---	
76		no	N/A	c.14251+1G>A	44	splicing error	+	chr12:47709110	
77		no	N/A	c.14710C>T	48	p.R4904X	+	chr12:47707306	
78		no	N/A	c.13895delC	42	p.P4632HfsX8	-	chr12:47710434	
79		no	N/A	c.16412G>C	52	p.R5471T	-	chr12:47702330	
80		no	N/A	c.6334delG	31	p.A2112HfsX32	+	chr12:47721486	
81		no	N/A	c.11821C>T	39	p.Q3941X	+	chr12:47712934	
82		no	N/A	c.8727_8730delAAGT	34	p.S2910RfsX32	-	chr12:47718676-79	
83		no	N/A	c.8721C>G	34	p.Y2907X	+	chr12:47718685	
84		no	N/A	c.12688C>T	39	p.Q4230X	+	chr12:47712067	
85		no	N/A	c.14946G>A	48	p.W4982X	+	chr12:47707070	
86		no	N/A	c.16437delT	53	p.N5480TfsX7	+	chr12:47702177	
87		no	N/A	c.11764C>T	39	p.Q3922X	-	chr12:47712991	
88		no	N/A	c.16489_16491delATC	53	p.I5497del	-	chr12:47702123-25	
89		no	N/A	c.15640C>T	48	p.R5214C	+	chr12:47706376	
90		no	N/A	c.8488C>T	34	p.R2830X	+	chr12:47718918	
91		no	N/A	c.9581delA	34	p.H3194PfsX3	-	chr12:47717825	
92		no	N/A	c.16489_16491delATC	53	p.I5497del	+	chr12:47702123-25	
93		no	N/A	---	---	---	---	---	
94		no	N/A	c.4288T>C	15	p.C1430R	-	chr12:47726789	
95		no	N/A	c.10395delA	36	p.P3466LfsX36	-	chr12:47714677	
96		no	N/A	---	---	---	---	---	
97		no	N/A	I	I	I	I	I	Two variants were found in this individual [c.4042C>T(+)c.4132-1G>A]. We could not determine which variant is pathogenic.
98		no	N/A	c.15536G>A	48	p.R5179H	-	chr12:47706480	
99		no	N/A	c.15640C>T	48	p.R5214C	-	chr12:47706376	
100		no	N/A	c.4163G>T	14	p.R1388L	-	chr12:47728088	
101		no	N/A	c.13201C>T	39	p.Q4401X	-	chr12:47711554	
102		no	N/A	c.11149C>T	39	p.Q3717X	-	chr12:47713606	
103		no	N/A	c.15339C>A	48	p.Y5113X	-	chr12:47706677	
104		no	N/A	c.16438_16441delAACT	53	p.N5480VfsX6	-	chr12:47702173-76	
105		no	N/A	---	---	---	---	---	
106		no	N/A	c.8665G>T	34	p.G2889X	-	chr12:47718741	
107		no	N/A	c.6594delC	31	p.Y2199IfsX65	-	chr12:47721226	
108		no	N/A	c.9961C>T	34	p.R3321X	-	chr12:47717445	
109		no	N/A	c.8859_8861delGGGinsCA	34	p.K2953NfsX51	-	chr12:47718545-47	
110		no	N/A	---	---	---	---	---	
111		no	N/A	c.8952delG	34	p.K2985SfsX19	-	chr12:47718454	

--- no mutation identified
\+ confirmed de novo
\- no parental samples available
X stop codon
fs frameshift
a chromosomal position was determined using March 2006 assembly from UCSC (hg18)
* confirmed as inherited
N/A not published previously by Ng, SB et al. [2010]
I inconclusive sequencing results

K33380	4786	57	no	c.C13285T	39	p.Q4429X	+	chr12:47711470
K34163	5937	58	no	c.C11423T - REAL???	39	p.A3808V - REAL???	+	chr12:47713332
K34221	6504	59	no	c.C11047T	39	p.Q3683X	-	chr12:47713708
K34222	6508	60	no	c.C7228TT	31	p.R2430X	-	chr12:
K34224	6513	62	no	--	--	--	--	--
K34225	6518	63	no	--	--	--	--	--
K34226	6520	64	no	c.?	31	p.P2550fs	-	chr12:
K34227	6522	65	no	c.G699del	6	p.G234fs	-	chr12:
K34228	6524	66	no	c.C16342T	52	p.R5448X	-	chr12:
K34229	6526	67	no	c.C16360T	52	p.R5454X	-	chr12:
K34230	6528	68	no	--	--	--	--	--
K34231	6530	69	no	c.C7228TT	27	p.R2430X	-	chr12:
K34232	6532	70	no	c.?	34	~p.H3283fs	-	chr12:
K34233	6535	71	no	c.?	48	p.M5029fs	-	chr12:
K34234	6538	72	no	c.C15142T	48	p.R5048C	-	chr12:
K34235	6540	73	no	c.G15641A	48	p.R5214H	-	chr12:
K34236	6543	74	no	--	--	--	--	--
K34530	6842	75	no	c.?	46	p.E4829fs	no mutation in mother / father not available	chr12:
K34531	6840	76	no	--	--	--	--	--
K34532	6838	77	no	G->A +1bp	44		+	chr12:
K34533	6835	78	no	c.C14710T	48	p.R4904X	+	chr12:
K34534	6832	79	no	c.C13891del	42	p.P4632fs	mother available	chr12:
K34535	6830	80	no	c.G16412C	52	p. R5471T	no mutation in mother / father not available	chr12:
K34536	6828	81	no	c.G6331del	31	p.A2112fs	father no mutation; redo mother	chr12:
K34537	6825	82	no	c.C11821T	39	p.Q3941X	+	chr12:47712934
K34538	6822	83	no	c.?	34	p.V2909fs	-	chr12:
K34539	6821	84	no	c.C8721G	34	p.Y2907X	+	chr12:
K34633	6744	85	no	c.C12688T	39	p.Q4230X	+	chr12:47712067
K34649	6794	86	no	c.G14946A	48	p.W4982X	+	chr12:
K34650	6795	87	no	c.T16437del	53	p.P5479fs	pending both parents collected	chr12:
K34651	6796	88	no	c.C11764T	39	p.Q3922X	-	chr12:47712991
K34652	6797	89	no	c.?	53	p.I5494fs	-	chr12:
K34653	6798	90	no	c.C15640T	48	p.R5214C	+	chr12:
K34654	6799	91	no	c.C8488T	34	p.R2830X	+	chr12:
K34655	6800	92	no	--	--	--	--	--
K34656	6801	93	no	c.?	53	p.I5494fs	pending both parents collected	chr12:
K34657	6802	94	no	--	--	--	--	--
K34658	6803	95	no	c.T4288C	15	p.C1430R	-	chr12:
K34659	6804	96	no	c.G10389del	36	p.S3463fs	-	chr12:
K34660	6805	97	no	--	--	--	--	--
K34661	6806	98	no	G->A -1bp	14	altered splicing	-	chr12:
K34662	6807	99	no	c.G15536A	48	p.R5179H	not available, de novo in #4480	chr12:
K34663	6808	100	no	c.C15640T	48	p.R5214C	-	chr12:
K34664	6809	101	no	c.G4163T	14	p.R1388L	-	chr12:
K34665	6810	102	no	c.C13201T	39	p.Q4401X	-	chr12:47711554
K34666	6811	103	no	c.C11149T	39	p.Q3717X	-	chr12:47713606
K34667	6812	104	no	c.C15339A	48	p.Y5113X	-	chr12:
K34668	6813	105	no	c.?	53	p.N5480fs	-	chr12:
K34669	6814	106	no	--	--	--	--	--
K34670	6815	107	no	c.G8665T	34	p.G2889X	-	chr12:
K34671	6816	108	no	c.?	31	p.P2198fs	-	chr12:
K34672	6817	109	no	c.C9961T	34	R3321X	-	chr12:
K34673	6818	110	no	c.?	34	K2953fs	-	chr12:
K34680	6876	111	no	--	--	--	--	--
K34681	6879	112	no	c.?	34	K2984fs	buccals pending	chr12:

Population Genetic Structure of Peninsular Malaysia Malay Sub-Ethnic Groups

Wan Isa Hatin[1], Ab Rajab Nur-Shafawati[1], Mohd-Khairi Zahri[1], Shuhua Xu[3], Li Jin[3], Soon-Guan Tan[5], Mohammed Rizman-Idid[4,6], Bin Alwi Zilfalil[1,2]*, The HUGO Pan-Asian SNP Consortium[¶]

1 Human Genome Centre, School of Medical Sciences, Universiti Sains Malaysia, Kelantan, Malaysia, **2** Department of Pediatrics, School of Medical Sciences, Universiti Sains Malaysia, Kelantan, Malaysia, **3** Chinese Academy of Sciences and Max Planck Society (CAS-MPG) Partner Institute for Computational Biology, Shanghai Institutes for Biological Sciences, Chinese Academy of Sciences, Shanghai, China, **4** Institute of Biological Sciences, Faculty of Science, Universiti Malaya, Kuala Lumpur, Malaysia, **5** Department of Cell and Molecular Biology, Faculty of Biotechnology and Biomolecular Sciences, Universiti Putra Malaysia, Selangor, Malaysia, **6** Centre of Research for Computational Sciences and Informatics in Biology, Bioindustry, Environment, Agriculture and Healthcare (CRYSTAL), Faculty of Science, Universiti Malaya, Kuala Lumpur, Malaysia

Abstract

Patterns of modern human population structure are helpful in understanding the history of human migration and admixture. We conducted a study on genetic structure of the Malay population in Malaysia, using 54,794 genome-wide single nucleotide polymorphism genotype data generated in four Malay sub-ethnic groups in peninsular Malaysia (*Melayu Kelantan, Melayu Minang, Melayu Jawa* and *Melayu Bugis*). To the best of our knowledge this is the first study conducted on these four Malay sub-ethnic groups and the analysis of genotype data of these four groups were compiled together with 11 other populations' genotype data from Indonesia, China, India, Africa and indigenous populations in Peninsular Malaysia obtained from the Pan-Asian SNP database. The phylogeny of populations showed that all of the four Malay sub-ethnic groups are separated into at least three different clusters. The *Melayu Jawa, Melayu Bugis* and *Melayu Minang* have a very close genetic relationship with Indonesian populations indicating a common ancestral history, while the *Melayu Kelantan* formed a distinct group on the tree indicating that they are genetically different from the other Malay sub-ethnic groups. We have detected genetic structuring among the Malay populations and this could possibly be accounted for by their different historical origins. Our results provide information of the genetic differentiation between these populations and a valuable insight into the origins of the Malay sub-ethnic groups in Peninsular Malaysia.

Citation: Hatin WI, Nur-Shafawati AR, Zahri M-K, Xu S, Jin L, et al. (2011) Population Genetic Structure of Peninsular Malaysia Malay Sub-Ethnic Groups. PLoS ONE 6(4): e18312. doi:10.1371/journal.pone.0018312

Editor: Henry Harpending, University of Utah, United States of America

Received October 7, 2010; **Accepted** March 3, 2011; **Published** April 5, 2011

Funding: This research was supported by Fundamental Research Grants Scheme (FRGS) project (Grant Number: 203/PPSP/6170025) and Universiti Sains Malaysia (USM) Fellowship Scheme. The funders had no role in study design, data collection and analysis, decision to publish, or preparation of the manuscript.

Competing Interests: The authors have declared that no competing interests exist.

* E-mail: zilfalil@kb.usm.my

¶ The HUGO Pan-Asian SNP Consortium authors with their affiliations are listed in Text S1.

Introduction

Malays (*Melayu*) are an ethnic group who speak Malayo-Polynesian language which is a member of the Austronesian family [1,2]. They predominantly inhabit the Malay Peninsula, the east coast of Sumatra and the coast of Borneo [1]. In Peninsular Malaysia, the Malays consist of various sub-ethnic groups which are believed to have different ancestral origins based on their migrations centuries ago [3]. The Malay Peninsula was once a very strategic port and trading centre, connecting Indochina and the Indonesian archipelago [4]. However, migrating populations from surrounding areas has further confounded the investigation of the origin of Malays.

This study aims to investigate whether the different Malay sub-ethnic groups originate from a single population or several populations by exploring the possibility of genetic structuring. The Malay populations in the western (*Melayu Minang*) and southern parts (*Melayu Jawa* and *Melayu Bugis*) of the Peninsular Malaysia were believed to have had more historical and cultural links with the populations from the Indonesian archipelago compared to the Malay populations in north-eastern regions (*Melayu Kelantan*). The existence of Chinese and Indian in the Malay Peninsula with different timelines throughout the centuries brought varying degrees of cultural influences and genetics admixtures to the Malay populations. Substantial influx of Chinese and Indians were started only during the British colonial era to work as laborers in the tin mines and the plantation industry that were mainly concentrated on the west coast of peninsula [5]. Prior to British colonization, Chinese and Indian traders had established strong trading links with the Malay Peninsula. These early contacts did not cause large scale migration but intermarriage and integration between them and the Malays were common [5]. Moreover, the Indians had been conspicuous in the region very much earlier, since the period of the ancient Hindu Malay kingdoms which arose in the 2nd century such as *Chi Tu, Gangga Negara, Kadaram* and *Langkasuka* that controlled much of the northern Malay Peninsula [6]. These early Malay states were heavily influenced by concepts of religion, government and arts that were brought by the Indians and traces of this influence can still be found in Malays culture despite the later influence of Islam [6,7].

In addition, the existence of indigenous *Orang Asli* (aboriginal peoples) populations in the peninsula such as the Negritos (*Jahai* and *Kensui*) and Proto-Malays (*Temuan*) have also raised questions as to whether they are associated with the first wave of human migration from Africa, or belong to the more recent events of Asian human evolution [8,9]. The Negritos, who speak the Aslian languages which are part of the Austro-Asiatic language family, are of Australo-Malesian affinity and share some common physical features with African pygmy populations, including short stature, woolly hair and dark skin [8,10]. These nomadic hunter-gatherers are believed to be the earliest settlers and original coastal inhabitants of the Malay Peninsula but the arrival of newcomers forced this group further inland, resulting in them being isolated in forested hilly regions, mainly in northern part of Peninsular Malaysia [10,11]. Meanwhile, the Proto-Malays who arrived later than Negritos in 2000 BC were seafaring people and settled mostly in the central and southern regions of Peninsular Malaysia [1,11]. They are Austronesian speakers apart from one tribe, (the *Semelai*) who speak Aslian [9] and embrace people who are similar in appearance to the Malays but of diverse origins, some probably having entered the region by sea in recent centuries whilst others may have been living in the peninsula for thousands of years [9,10]. In contrast, the present-day Malays of the Malay Peninsula are described as Deutero-Malays, the descendants of the Proto-Malays who had admixed with Siamese, Javanese, Sumatran, Indian, Thai, Arab and Chinese traders [12]. However, according to Fix [10], the original Deutero-Malays migrated from southern China (after the migration of the Proto-Malays) over 1500 years ago and their intermarriages with the Proto-Malays and traders of the ancient trade routes resulted in the diverse recent Deutero-Malay populations that became known currently as the Malays. Hence, Malay population structure analysis would not just provide the information on the genetic differentiation between the populations but would also provide insight into the relationship with the indigenous populations in Peninsular Malaysia.

In this study, we used single nucleotide polymorphisms (SNPs) due to their amenability to high throughput genotyping [13]. SNPs are valuable genetic markers for revealing the evolutionary history of populations [14,15,16]. In this analysis more than 54,000 SNPs loci that were shared by 434 individuals were screened to investigate the distribution of genetic variation and population genetic structure of the Malay populations. This number is sufficient to estimate population genetic parameters with statistical confidence [14,17].

The distance-based approaches that are used in this analysis can detect fine-scale population structure of our studied populations and are not computationally demanding compared to model-based approaches [18]. Inference based on this method does not depend on the modeling assumptions and also requires no special marker selection criteria. In addition, the SNPs analyses with distance-based method are very fast, efficient, robust and able to handle relatively small sample sizes, especially when investigating isolated populations that comprised of few individuals [18,19,20]. We implemented these methods to investigate the population genetic structure of four Malay sub-ethnic groups; *Melayu Kelantan*, *Melayu Minang*, *Melayu Jawa*, and *Melayu Bugis* in Peninsular Malaysia. We included the indigenous Proto-Malay and Negrito populations to determine the degree of their genetic relatedness to the Malays.

Materials and Methods

The population sampling of Peninsular Malaysia Malays were done by following the inclusion and exclusion criteria (Table 1). The SNPs genotype data of 71 unrelated individual of four Malay sub-ethnic groups namely Melayu Kelantan, Melayu Minang, Melayu Jawa and Melayu Bugis were generated by Affymetrix GeneChip Mapping Xba 50 K Array, a microarray chip that enabled researchers to screen over 50,000 SNPs loci in each individual. A total of 58,960 SNPs that have been genotyped for all the sampled individuals were screened under the strict criteria of data quality control. Samples with a call rate below than 90% were excluded from further analysis and after the assessment, 4,166 SNPs (7%) were filtered out (Unmapped to Affymetrix annotation file, chromosome X SNPs and intersection SNPs with downloaded Pan-Asian SNP genotypes), leaving a total of 54,794 autosomal SNPs as the final genotype data for each individual to be used in further analyses.

The additional 11 populations (Table 1) comprised of Proto-Malays (*Temuan*), Negritos (*Jahai* and *Kensui*), Indonesian Malays (*Melayu*, *Jawa* and *Toraja*), Yunnan Chinese (*Jinuo* and *Wa*), South-West Indians (who speak in *Marathi* and *Telegu* language) and Africans (*Yoruba*) were obtained from the Pan-Asian SNP database [21] (http://www4a.biotec.or.th/PASNP). All of these genotype data were generated from DNA samples that were collected with informed and written consent and approved by local ethics committees (Research and Ethics (Human) Committee, School of Medical Sciences, Universiti Sains Malaysia (USM)) and institutional review board (IRB) of the respective countries.

Table 1. List of all studied populations with the location and sample ID.

Population (No. of samples)	Sample ID	Location
Malaysian Melayu[a]:		Peninsular Malaysia:
Kelantan (18)	MY-KN	Kelantan
Minang (20)	MY-MN	Negeri Sembilan
Jawa (19)	MY-JV	Johor
Bugis (14)	MY-BG	Johor
Proto-Malay[b]:		
Temuan (49)	MY-TM	Negeri Sembilan
Negrito[b]:		
Jahai (50)	MY-JH	Perak
Kensui (30)	MY-KS	Kedah
Indonesian[b]:		Indonesia:
Melayu (12)	ID-ML	Sumatra
Jawa (19)	ID-JV	Java Island
Toraja (20)	ID-TR	Sulawesi
Chinese[b]:		China:
Jinuo (29)	CN-JN	Yunnan
Wa (56)	CN-WA	Yunnan
Indian[b]:		India:
Marathi (14)	IN-WL	Maharashtra
Telugu (24)	IN-DR	Andhra Pradesh
African[b]:		Africa:
Yoruba (60)	YRI	Nigeria

[a]The inclusion criteria are; the sampled individual of a population must be at least three generations of the same population, no parental admixture and communicate daily in the local dialect. The exclusion criteria are those that contradict the inclusion criteria.

[b]The genotype data that were obtained from the Pan-Asian SNP Consortium database.

doi:10.1371/journal.pone.0018312.t001

Allele frequency and genetic distance based on Fixation Index Statistic (Fst) [22] were calculated by PEAS v1.0 [23]. MEGA 4 software [24] and two programs, Neighbor and Consense from PHYLIP 3.67 [25], were implemented to construct the Neighbor Joining tree [26] using all 54,794 autosomal SNPs, shared by 434 individuals from 15 populations. The tree was rooted using *Yoruba* (YRI) as outgroup. Bootstrapping test was performed 1000 times, whereby branches with less than 80% bootstrap values have been dissolved. Multi-dimensional scale analysis was done by SPSS 13 and represented in Euclidean distance three dimension (3D) model.

Results and Discussion

Fst [22] is a method to show population genetic structure by partitioning genetic variance within populations relative to between populations. The Neighbor Joining tree (Figure 1) based on the genetic distance measure of Fst for the 15 studied populations showed strongly supported nodes (>95% of bootstrap values) and was rooted using *Yoruba* (YRI) as an outgroup. *Yoruba* is an ethnic group from Nigeria and serve as an outgroup to the non-African populations in our study. As the sampling procedure stringently followed the inclusion and exclusion criteria that emphasized the three generations without any different ethnic admixture rule for an individual to be considered as a valid subject for this study, we assumed that there was no recent admixture or gene flow among all the studied populations.

In the Fst tree (Figure 1), each of the Malay sub-ethnic groups in Peninsular Malaysia; *Melayu Kelantan* (MY-KN), *Melayu Minang* (MY-MN), *Melayu Jawa* (MY-JV) and *Melayu Bugis* (MY-BG) is monophyletic, thus establishing there is substructure among Malays. However, the tree does not support the designation of Malays as a monophyletic group since the MY-KN were on a separated clade from other Malay populations, and the MY-JV were more closely related to Proto-Malays and Chinese than other

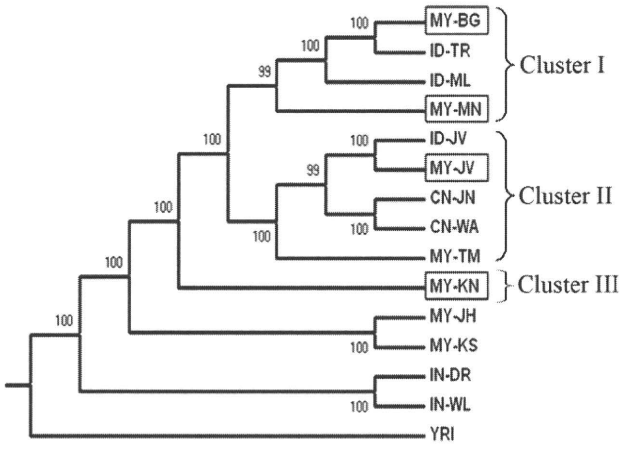

Figure 1. Neighbor-Joining tree of 15 populations based on Fst measurement. In the square boxes are the four studied Malay sub-ethnic groups. Numbers at each branch are represent the percentage value of a thousand bootstrap replications and branches with bootstrap values less than 80% were condensed. The tree suggests a diverse origin of the Malay sub-ethnic groups that forms Cluster I, II and III. Notably, the position of MY-KN in Clade III is the most basal among other studied Malays supported by 100% of bootstrap replicates. There is a distinct genetic difference between the indigenous *Orang Asli* populations; the Negritos is oldest among the peopling groups in Malay Peninsula, whereas the Proto-Malays shared a common ancestry or have had some mixing with the Chinese and Javanese populations.
doi:10.1371/journal.pone.0018312.g001

Malays. Generally, the populations were assigned into three different clusters (Cluster I, II, and III) instead of forming a single Malays cluster. Different ancestry across the Malay groups is likely, as they are a paraphyletic class.

In Cluster I, the MY-MN was grouped with Indonesian *Melayu* (ID-ML), whereas MY-BG was grouped with Indonesian *Toraja* (ID-TR). The topology may reflect the migrations of MY-MN and MY-BG to Malay Peninsula from Sumatra and Sulawesi, which are also the geographic origins of ID-ML and ID-TR, respectively. Between these populations, MY-MN appeared as the more basal group than MY-BG, which may suggest populations in Sumatra may have separated earlier than those in Sulawesi.

Cluster II grouped the *Melayu Jawa* (MY-JV) together with Indonesian *Jawa* (ID-JV), which suggest past migration between these populations, or common ancestry. Both populations cluster with the Chinese groups (CN-JN and CN-WA). The Chinese may have had more widespread admixture with the *Jawa* people rather than other Malays, Malaysian and Indonesian in this study. As both Malaysian and Indonesian *Jawa* have very close genetic relationship with the Chinese, it could be postulated that the mixture happened before the migration event of the *Jawa* people to Malay Peninsula around 15th century [27].

In Cluster III, the *Melayu Kelantan* (MY-KN) were basal compared to other Malays on the tree. Interestingly it formed an independent clade and placed outside, rather than within the two mentioned clades. The topology might suggest that MY-KN may have had an ancestry that is more divergent than those of the other Malay populations. This could also be attributed to their geographical location at the northern part of Peninsular Malaysia, which would account for their limited links with populations from the Indonesian archipelago. In contrast, MY-MN, MY-BG and MY-JV, have settled on the western and southern regions of the peninsula in proximity to the Indonesian archipelago.

The other explanation for the paraphyletic nature of the Malay class could be admixture of MY-KN with Indian populations (represented by IN-DR and IN-WL). The influence of Hinduism from India was historically very great and the Malays were largely 'Indianized' before they were converted to Islam [7]. Although Hinduism also existed in some of the Indonesian islands (eg. Java Island), it was more predominant among the cultures of populations in mainland Southeast Asia such as Thailand, Cambodia, Myanmar which had more direct contact with the Indian populations [28]. And, the northern part of Peninsular Malaysia had more historical connections with these civilizations [7,29] since centralization of the ancient Indianized kingdoms had occurred in that region for centuries in the early millennium.

Possible admixture between Malays and Indians was first shown genetically using biochemical markers [30]. Even though the admixture could have occurred during the British colonial period from the 19th to the middle of the 20th century when massive migration of Indian laborers to the west coast of Peninsular Malaysia to work on the railroad and in the rubber and oil palm plantation industries took place [5], we believed that the admixture between MY-KN and Indians was very ancient and had happened during the early existence of the Malays. According to the 2010 Malaysian population census, Malaysia's population is about 28.9 million and the Indian community is the smallest of the three main ethnic groups, comprising 6.8% of the population, with most of them residing in the western and north-western regions of Peninsular Malaysia which are the location of the big cities and large urban areas in the country. In Kelantan state which is the origin of MY-KN, the total population is about 1.67 million and the percentage of the Indian community is only 0.2% of the population. The Indians are not a large component of the

Kelantan population either during or after the British colonial era, as it is an agrarian state with lush paddy fields and rustic fishing villages without any plantation industry to attract the Indian immigrants to this north-eastern part of the peninsula [5].

Regarding the phylogenetic affinities of aboriginal peoples in Malaysia, it was revealed that the Proto-Malay, *Temuan* (MY-TM) population was more related to the Chinese and Malays, especially with *Jawa* populations than the Negritos, represented by the *Kensui* (MY-KS) and *Jahai* (MY-JH) populations. This topology is consistent with the fact that the tribal Proto-Malays are believed to have migrated from Yunnan, China about 4,000–6,000 years ago [1]. They were once probably people of coastal Borneo who expanded into Sumatra and the Malay Peninsula as a result of their seafaring way of life [2,31]. Thus, our results may provide a genetic evidence of the pre-historic migration of Proto-Malays from Yunnan, China.

On the other hand, the Negritos are regarded as the earliest inhabitants of the Malay Peninsula and are probably descended from the Hoabinhians, as their mtDNA variation shows strong evidence for indigenous origins within Malay Peninsula, with time depth of ~60,000 years ago [9,32]. However, their origin and the route of their migration to Asia is still a matter of great speculation [33,34]. Nevertheless, the suggestion of their origin via a southern route of migration from South India is also plausible, as the recent mtDNA studies on 'relict' populations of Southeast Asia and the Andaman and Nicobar Islands also point to the human dispersals through the southern exit route [32,35,36]. The phylogenetic tree showed a concordance with the facts mentioned above, where the position of the Negritos on the tree were placed at the most basal position among the Malay, Indonesian and Chinese populations. The genetic relationship of the Malays and aboriginal peoples has not only provided some additional insight to the initial peopling in Malay Peninsula, but also may allow one to gauge admixture due to more recent migration.

The genetic structure of Malays in the Fst tree is recapitulated by multi dimensional scale (MDS) analysis in three dimensions (3D) model as shown in Figure 2. Notably, all four Malay sub-ethnic groups are well separated into three different sub-clusters, although they still remained in the same dimensional platform (dimension 3) indicating an existence of substructure within the Malay population. Malay sub-ethnic groups clustered together with Chinese populations (CN-JN and CN-WA) on the middle area of the dimension 3 platform and far separated from three other group populations which are *Yoruba*, Indians (IN-DR and IN-WL) and Negritos (MY-JH and MY-KS) which are far more diversified than the modern Malays.

Conclusion

One of the goal of population genetics to understand the nature and extent of human population structure [37]. We have utilized the distance-based clustering method to show the population genetic structure of Malays and the existence of differences among them. The detected substructure of Malays of Peninsular Malaysia indicates the existence of genetic heterogeneity in the population that might relate to the diverse origins and histories. This study has performed investigation of more comprehensive Malay populations that were not included in the report by Pan-Asian SNP research (PASNPI) [21]. The inclusion of the indigenous populations in this study have shown genetic affinities which have not been revealed in previous studies.

Our results illustrate the potential to investigate further the peopling of Peninsular Malaysia by including more ethnic groups not covered in this study. For a culturally mixed country such as

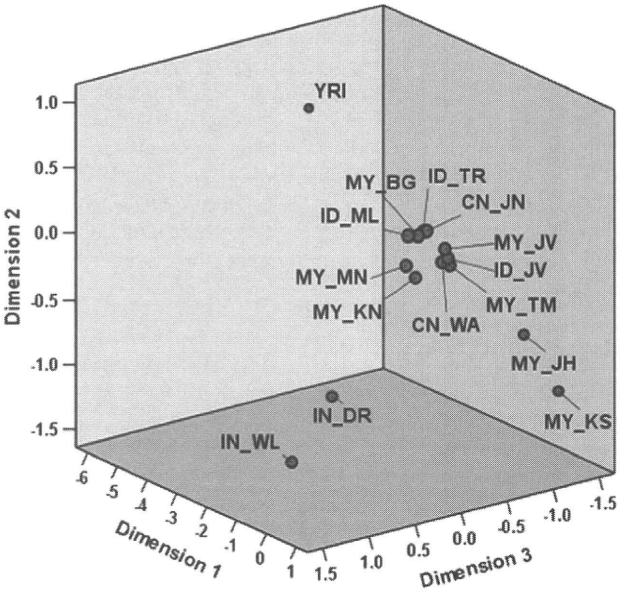

Figure 2. MDS analysis in three dimension model recapitulated the pattern of Fst tree. The 3D MDS showed that all four Malay populations are well separated into three different sub-clusters, although still remained in the same cluster and dimensional platform. They are far separated from three other group populations which are Yoruba, Indian (IN-DR and IN-WL) and Negrito (MY-JH and MY-KS) which are far more diversified than the modern Malays.
doi:10.1371/journal.pone.0018312.g002

Malaysia, where people of various ethnicity practice different lifestyles under many different environments, the knowledge of population genetic substructure is important for proper design of case control association studies and for identifying disease predisposing alleles that may differ across ethnic groups [38]. Only by characterizing genetic variation among individuals and populations, can we gain a better understanding of differential susceptibility to disease, differential response to pharmacological agents and complex interaction of genetic and environmental factors in producing phenotypes [38].

Supporting Information

Text S1 The participants of the HUGO Pan-Asian SNP Consortium are arranged alphabetically by surname.
(DOC)

Acknowledgments

We acknowledged the contributions by the other members of this study group from the School of Health Sciences and the School of Dental Sciences, Universiti Sains Malaysia. We thank all the subjects who have participated in this research and those who have helped us in the data collection. Special thanks to the UKM Medical Molecular Biology Institute (UMBI), Universiti Kebangsaan Malaysia and Matrix Analytical Sdn. Bhd., Malaysia for allowing us to use their laboratory facilities.

Author Contributions

Conceived and designed the experiments: NSAR ZMK PASNPI. Performed the experiments: NSAR ZMK PASNPI. Analyzed the data: HWI. Contributed reagents/materials/analysis tools: SX LJ PASNPI. Wrote the paper: HWI. Population sampling: NSAR HWI ZBA PASNPI. Interpretation of results: HWI SX RIM. Critical review of manuscript: TSG ZBA RIM SX LJ HWI NSAR.

References

1. Bellwood PS (1997) Prehistory of the Indo-Malaysian Archipelago. Honolulu, Hawaii: University of Hawai'i Press. x, 384 p., [340] p. of plates p.
2. Omar AH (2004) Languages and Literature. The Encyclopedia of Malaysia.
3. Paul W (1961) The Golden Khersonese: Studies in the Historical Geography of the Malay Peninsula before AD 1500. Kuala Lumpur: University of Malaya Press.
4. Jacq-Hergoualc'h M, Hobson V The Malay Peninsula: Crossroads of the Maritime Silk Road (100 BC-1300 AD): BRILL. 607 p.
5. (2008) Malaysia, Singapore, Brunei, and the Philippines. New York: Marshall Cavendish Reference. 1584 p.
6. Arasaratnam S Indians in Malaysia and Singapore: Published for the Institute of Race Relations, London, by Oxford University Press (Bombay). 214 p.
7. I Syukri (2002) Sejarah Kerajaan Melayu Patani/Ibrahim Syukri. Bangi: Universiti Kebangsaan Malaysia. pp 131, 129.
8. Allen FA (1879) The Original Range of The Papuan and Negrito Races. The Journal of the Anthropological Institute of Great Britain and Ireland 8: 38–50.
9. Hill C, Soares P, Mormina M, Macaulay V, Meehan W, et al. (2006) Phylogeography and ethnogenesis of aboriginal Southeast Asians. Mol Biol Evol 23: 2480–2491.
10. Fix AG (1995) Malayan paleosociology: implications for patterns of genetic variation amongst the Orang Asli. American Anthropology 97: 313–323.
11. Carey I (1976) Orang Asli: the aboriginal tribes of peninsular Malaysia. Kuala Lumpur; New York: Oxford University Press.
12. Comas D, Calafell F, Mateu E, Perez-Lezaun A, Bosch E, et al. (1998) Trading genes along the silk road: mtDNA sequences and the origin of central Asian populations. Am J Hum Genet 63: 1824–1838.
13. Brookes AJ (1999) The essence of SNPs. Gene 234: 177–186.
14. Brumfield RT, Beerli P, Nickerson DA, Edwards SV (2003) The utility of single nucleotide polymorphisms in inferences of population history. TRENDS in Ecology and Evolution 18: 249–256.
15. Kuhner MK, Beerli P, Yamato J, Felsenstein J (2000) Usefulness of single nucleotide polymorphism data for estimating population parameters. Genetics 156: 439–447.
16. Petkovski E, Keyser C, Ludes B, Hienne R (2003) Validation of SNPs as markers for individual identification. International Congress Series 1239: 33–36.
17. Nielsen R (2000) Estimation of population parameters and recombination rates using single nucleotide polymorphisms. Genetics 154: 931–942.
18. Gao X, Starmer J (2007) Human population structure detection via multilocus genotype clustering. BMC Genet 8: 34.
19. Mihaescu R, Levy D, Pachter L (2009) Why Neighbor-Joining Works. Algorithmica 54: 1–24.
20. Crandall K, Lagergren J, Simonsen M, Mailund T, Pedersen C (2008) Rapid Neighbour-Joining. Algorithms in Bioinformatics: Springer Berlin/Heidelberg. pp 113–122.
21. The-HUGO-Pan-Asian-SNP-Consortium (2009) Mapping Human Genetic Diversity in Asia. Science 326: 1541–1545.
22. Weir BS, Hill WG (2002) Estimating F-statistics. Annu Rev Genet 36: 721–750.
23. Xu SH, Gupta S, Jin L (2010) PEAS V1.0: a package for elementary analysis of SNP data. Molecular Ecology Resources 10: 1085–1088.
24. Tamura K, Dudley J, Nei M, Kumar S (2007) MEGA4: Molecular Evolutionary Genetics Analysis (MEGA) software version 4.0. Mol Biol Evol 24: 1596–1599.
25. Felsenstein J (2007) PHYLIP: Phylogeny Inference Package. University of Washington.
26. Saitou N, Nei M (1987) The neighbor-joining method: a new method for reconstructing phylogenetic trees. Mol Biol Evol 4: 406–425.
27. Taylor JG, ebrary Inc (2003) Indonesia peoples and histories. New Haven: Yale University Press. p xxi, 420.
28. Wolters OW, Reynolds CJ, Cornell University. Southeast Asia P (2008) Early Southeast Asia: selected essays. Ithaca, New York: Southeast Asia Program, Cornell University.
29. Allen SJ (1998) History, Archaeology, and the Question of Foreign Control in Early Historic-Period Peninsular Malaysia. International Journal of Historical Archaeology 2: 261–289.
30. Teng YS, Tan SG (1979) Genetic evidence of gene flow from Indians to Malays. Journal of Human Genetics 24: 1–8.
31. Rahman NHSNA (1998) Early History. Encyclopedia of Malaysia. 46 p.
32. Macaulay V, Hill C, Achilli A, Rengo C, Clarke D, et al. (2005) Single, rapid coastal settlement of Asia revealed by analysis of complete mitochondrial genomes. Science 308: 1034–1036.
33. Consortium THP-AS (2009) Mapping human genetic diversity in Asia. Science 326: 1541–1545.
34. Kashyap V, Sitalaximi T, Sarkar B, Trivedi R (2003) Molecular relatedness of the aboriginal groups of Andaman and Nicobar Islands with similar ethnic populations. The International Journal of Human Genetics 3: 5–11.
35. Majumder PP (2008) Genomic inferences on peopling of south Asia. Curr Opin Genet Dev 18: 280–284.
36. Thangaraj K, Chaubey G, Kivisild T, Reddy AG, Singh VK, et al. (2005) Reconstructing the origin of Andaman Islanders. Science 308: 996.
37. Bamshad MJ, Wooding S, Watkins WS, Ostler CT, Batzer MA, et al. (2003) Human population genetic structure and inference of group membership. Am J Hum Genet 72: 578–589.
38. Tishkoff SA, Kidd KK (2004) Implications of biogeography of human populations for 'race' and medicine. Nature Genetics 36.

Death effector domain–containing protein (DEDD) is required for uterine decidualization during early pregnancy in mice

Mayumi Mori,[1] Miwako Kitazume,[1] Rui Ose,[2] Jun Kurokawa,[1] Kaori Koga,[3] Yutaka Osuga,[3] Satoko Arai,[1] and Toru Miyazaki[1]

[1]Laboratory of Molecular Biomedicine for Pathogenesis, Center for Disease Biology and Integrative Medicine, Faculty of Medicine, The University of Tokyo, Bunkyo-ku, Tokyo, Japan. [2]Department of Human Genome Research, Kazusa DNA Research Institute, Kisarazu, Chiba, Japan. [3]Department of Obstetrics and Gynecology, Faculty of Medicine, The University of Tokyo, Bunkyo-ku, Tokyo, Japan.

During intrauterine life, the mammalian embryo survives via its physical connection to the mother. The uterine decidua, which differentiates from stromal cells after implantation in a process known as decidualization, plays essential roles in supporting embryonic growth before establishment of the placenta. Here we show that female mice lacking death effector domain–containing protein (DEDD) are infertile owing to unsuccessful decidualization. In uteri of *Dedd*$^{-/-}$ mice, development of the decidual zone and the surrounding edema after embryonic implantation was defective. This was subsequently accompanied by disintegration of implantation site structure, leading to embryonic death before placentation. Polyploidization, a hallmark of mature decidual cells, was attenuated in DEDD-deficient cells during decidualization. Such inefficient decidualization appeared to be caused by decreased Akt levels, since polyploidization was restored in DEDD-deficient decidual cells by overexpression of Akt. In addition, we showed that DEDD associates with and stabilizes cyclin D3, an important element in polyploidization, and that overexpression of cyclin D3 in DEDD-deficient cells improved polyploidization. These results indicate that DEDD is indispensable for the establishment of an adequate uterine environment to support early pregnancy in mice.

Introduction

Approximately 10%–15% of couples experience infertility during their reproductive years, owing mainly to implantation failure. Among the reasons underlying such failure, defective development of functional decidua at the implantation site within the uterus has recently been highlighted (1–3). In response to implantation, stromal cells immediately surrounding the mucosal crypt where the embryo is embedded proliferate extensively and undergo differentiation into polyploid decidual cells, forming an avascular primary decidual zone, followed by a broad, well-vascularized secondary decidual zone. It is believed that this decidual structure is important for the provision of nutrition to the developing embryo and also acts as a barrier against uncontrolled trophoblast proliferation until the placenta develops. Analyses of mutant mice that show female infertility, such as in knockout mice for homeobox A10 (*Hoxa10*) (4, 5) or IL-11 receptor (6), have contributed to the investigation of the molecular mechanisms involved in decidualization. Recent evidence has implicated cell-cycle regulation as being essential for both the proliferation and differentiation of stromal cells. In particular, Das and colleagues reported that cyclin D3–dependent activation of cyclin-dependent kinase 4 (Cdk4) or Cdk6 appears to be involved sequentially in those two events during decidua formation (7). In addition to these essential elements, in this report, we present data indicating that the death effector domain–containing (DED-containing) protein DEDD is indispensable for the maturation of decidual cells and support of female fertility in mice.

We previously found that the DEDD protein, initially described as a member of the DED-containing protein family, is associated with the Cdk1/cyclin B1 complex, thereby decreasing the kinase activity of Cdk1 (8). This response impedes Cdk1-dependent mitotic progression, preserving synthesis of ribosomal RNA (rRNA) and protein and resulting in sufficient cell growth before cell division (8, 9). Consistently, depletion of DEDD results in a shortened mitotic duration, an overall decrease in the amount of cellular rRNA and protein, and decreased cell and body size (8, 9). In addition to the function of DEDD as a cell-cycle regulator, we recently determined that DEDD associates with S6K1 (10) and Akt (11), major elements of the signaling cascade involving mitogen-related PI3K. Such associations support the roles of S6K1 activity and Akt protein stability, respectively, in contributing to the maintenance of glucose homeostasis in the body (10, 11). Hence, DEDD is multifunctional and is involved in different physiological mechanisms. In fact, we found that female *Dedd*$^{-/-}$ mice are infertile, and embryos of all DEDD genotypes die during early pregnancy within the *Dedd*$^{-/-}$ uterus, whereas *S6K1*$^{-/-}$ female mice, which also show a similar small phenotype and attenuated glucose homeostasis, show normal fertility (12). Given the phenotypic similarity of *Dedd*$^{-/-}$ mice to other infertile mutant mice (4–6), this observation led us to address whether DEDD might also be involved in uterine decidualization.

In the present study, we assessed embryos implanted in *Dedd*$^{-/-}$ uteri. In addition, we analyzed the maturation state of uterine decidual cells from *Dedd*$^{-/-}$ mice in vitro and in vivo. We also studied the molecular mechanism underlying the inefficient decidualization of *Dedd*$^{-/-}$ cells.

Results

Female Dedd$^{-/-}$ *mice are infertile.* We found that *Dedd*$^{-/-}$ female mice exhibited complete sterility when mated with males of any genotype (*Dedd*$^{-/-}$, *Dedd*$^{+/-}$, or *Dedd*$^{+/+}$), although *Dedd*$^{-/-}$ offspring were born from the intercross of *Dedd*$^{+/-}$ mice at a Mendelian ratio, and

Conflict of interest: The authors have declared that no conflict of interest exists.
Citation for this article: *J Clin Invest.* 2011;121(1):318–327. doi:10.1172/JCI44723.

Table 1
Female *Dedd*$^{-/-}$ mice are infertile

Genotype		Offspring					
Female	Male	+/+	+/–	–/–	Sum	*n*	Birth rate
+/+	+/–	13 (46%)	15 (54%)	0 (0%)	28	6	4.67
+/+	–/–	0 (0%)	87 (100%)	0 (0%)	87	18	4.83
+/–	+/+	24 (51%)	23 (49%)	0 (0%)	47	10	4.70
+/–	+/–	108 (30%)	183 (51%)	66 (19%)	357	65	5.49
+/–	–/–	0 (0%)	47 (64%)	27 (36%)	74	17	4.35
–/–	+/+	0	0	0	0	23	0.00
–/–	+/–	0	0	0	0	37	0.00
–/–	–/–	0	0	0	0	12	0.00

The breeding efficiency in male-female combinations of various DEDD genotypes was investigated. Sum, total number of newborns; *n*, number of successful matings (with a vaginal plug); birth rate: sum/*n*.

Dedd$^{-/-}$ male mice were fertile (Table 1). Mating efficiency was comparable in female *Dedd*$^{-/-}$ mice and female mice of other genotypes, as assessed by vaginal plug formation (data not shown). The uterine *Dedd* mRNA level was upregulated after 4.5 dpc as assessed by quantitative RT-PCR (QPCR) (Figure 1A). An increase in *Dedd* expression was also observed in stromal cells differentiated to mature decidual cells in vitro in the presence of estrogen, progesterone (P4), and heparin-binding EGF-like growth factor (HB-EGF) (Figure 1B). Upregulation of *DEDD* expression along with the decidualization was also detected in human uterine stromal cells (Figure 1C). These results suggested that uterine DEDD is important after implantation and that the maturation of uterine decidual cells may be associated with DEDD expression.

Consistently, when 4.5-dpc uteri were analyzed with injection of blue dye (1% Chicago blue solution) (13), the number of implantation sites was comparable in *Dedd*$^{-/-}$ and *Dedd*$^{+/+}$ mice (6.8 ± 0.73 in *Dedd*$^{-/-}$ mice and 7.4 ± 0.40 in *Dedd*$^{+/+}$ mice; $n = 5$ each). In addition, the spacing and crowding of implanted embryos in the uterus was also similar in *Dedd*$^{-/-}$ and *Dedd*$^{+/+}$ mice (Figure 1D). Histologic analysis of 4.5-dpc *Dedd*$^{-/-}$ uteri revealed normal embryonic implantation (Figure 1E). No difference was observed in the size of the edematous region and the decidual zone, which are formed in response to implantation (Figure 1E). Immunostaining for COX-2, an implantation site marker (14), corroborated the finding of normal embryonic implantation in *Dedd*$^{-/-}$ and *Dedd*$^{+/+}$ uteri (Figure 1E). Similarly, the mRNA level for *Ptgs2/Cox2* was comparable in *Dedd*$^{-/-}$ and *Dedd*$^{+/+}$ uteri, as assessed by QPCR with total RNA isolated from implantation sites (data not shown). However, anatomical analysis showed that in *Dedd*$^{-/-}$ uteri, the number of living embryos decreased rapidly between 5.5 and 8.5 dpc (Figure 1F). At 9.5 dpc, the period of placenta formation, no living embryos were detected in *Dedd*$^{-/-}$ uteri (Figure 1F). During this period, living embryos in *Dedd*$^{-/-}$ uteri were of smaller size compared with those in *Dedd*$^{+/+}$ uteri, and the difference in average embryo size between these two groups became more prominent at later dpc (Table 2). Thus, whereas implantation occurred normally in *Dedd*$^{-/-}$ uteri, embryos showed growth defects and died by 9.5 dpc, before placenta formation. Note that serum levels of estrogen and P4, as well as mRNA levels for the receptor for each hormone (*Esr1* and *Pgr*, respectively) were similar in *Dedd*$^{-/-}$ and *Dedd*$^{+/+}$ females (Supplemental Figure 1; supplemental material available online with this article; doi:10.1172/JCI44723DS1). Preimplantation uterine histology was also comparable (Supplemental Figure 2). In addition, the proliferation of uterine epithelial and stromal cells as well as expression induction of genes such as *Vegf* and *Lif* in response to estrogen were similar in *Dedd*$^{-/-}$ and *Dedd*$^{+/+}$ ovariectomized mice (Supplemental Figure 3). In addition, histologic ovarian morphology, ovulation, and intrauterine fertilization were normal in *Dedd*$^{-/-}$ females (data not shown).

Defective decidualization and disintegrated structure of the implantation site in Dedd$^{-/-}$ *uteri.* Histological analysis of 5.5-dpc uteri showed that the size of the decidual zone was smaller in *Dedd*$^{-/-}$ compared with *Dedd*$^{+/+}$ mice (Figure 2A). This was confirmed by immunostaining for the decidua marker tissue inhibitor of metalloproteinase 3 (TIMP3) (quantification also shown in Figure 2A) (15). Consistent with these results, mRNA levels for various genes that are highly expressed in decidual cells were decreased in *Dedd*$^{-/-}$ compared with *Dedd*$^{+/+}$ uteri, as assessed by QPCR with total RNA isolated from implantation sites (Figure 2B). Of these, the expression level of P4-sensitive bone morphogenetic protein 2 (*Bmp2*) gene was compromised at 5.5 d.p.c in *Dedd*$^{-/-}$ uteri, whereas that of *Hoxa10*, upstream of *Bmp2* (5, 16, 17), was similar to that in *Dedd*$^{+/+}$ uteri. In addition to the decidual zone, the size of the edematous region surrounding the decidual zone was also decreased in *Dedd*$^{-/-}$ compared with *Dedd*$^{+/+}$ mice (Figure 2A), suggesting that vascular permeability might be reduced in *Dedd*$^{-/-}$ uteri.

Such attenuated development of the decidual zone in *Dedd*$^{-/-}$ uteri was accompanied by disintegrated structure of the implantation site at later phases of pregnancy. At 7.5 dpc, a large proportion of decidual cells exhibited a shrunken shape, and marked bleeding was detected at the edge of the cavity in *Dedd*$^{-/-}$ uteri (Figure 2C). In 8.5-dpc *Dedd*$^{-/-}$ uteri, the structure of the outer wall of the embryonic cavity, which is supported by Reichert's membrane and trophoblastic giant cells (TGCs), had collapsed (Figure 2C), and irregular distribution of TGCs (i.e., invasion of TGCs into inner area of uteri) was more remarkable (Figure 2D). Such inadequate uterine environment may cause infertility in female *Dedd*$^{-/-}$ mice.

Defective polyploidy in Dedd$^{-/-}$ *decidual cells.* We next assessed the state of polyploidy, a hallmark of mature decidual cells, in *Dedd*$^{-/-}$ and *Dedd*$^{+/+}$ uterine stromal cells undergoing decidualization in vitro in the presence of estrogen, P4, and HB-EGF. As shown in Figure 3A, at days 3 and 7, the proportion of multinuclear cells observed microscopically was more than 50% smaller in *Dedd*$^{-/-}$ cells than in *Dedd*$^{+/+}$ cells. Consistent with this result, analysis of these cells by the flow cytometer after DNA staining revealed a significant decrease in the proportion of cells that possessed more than 4 copies of genomic DNA (indicated as 4n and 8n) in *Dedd*$^{-/-}$ compared with *Dedd*$^{+/+}$ cells (Figure 3B). Similar results were obtained in vivo in cells isolated from 4.5-dpc implantation sites in *Dedd*$^{-/-}$ and *Dedd*$^{+/+}$ uteri by collagenase treatment (Figure 3C). Thus, the defect in decidualization observed in *Dedd*$^{-/-}$ uteri was associated with attenuated terminal maturation with less polyploidy.

In contrast, the proliferative status of uterine stromal cells in response to implantation was not different in *Dedd*$^{-/-}$ and *Dedd*$^{+/+}$ mice, as judged by the comparable cell number isolated from implantation sites at 4.5 dpc ($1.08 \times 10^6 \pm 0.15 \times 10^6$ in *Dedd*$^{-/-}$

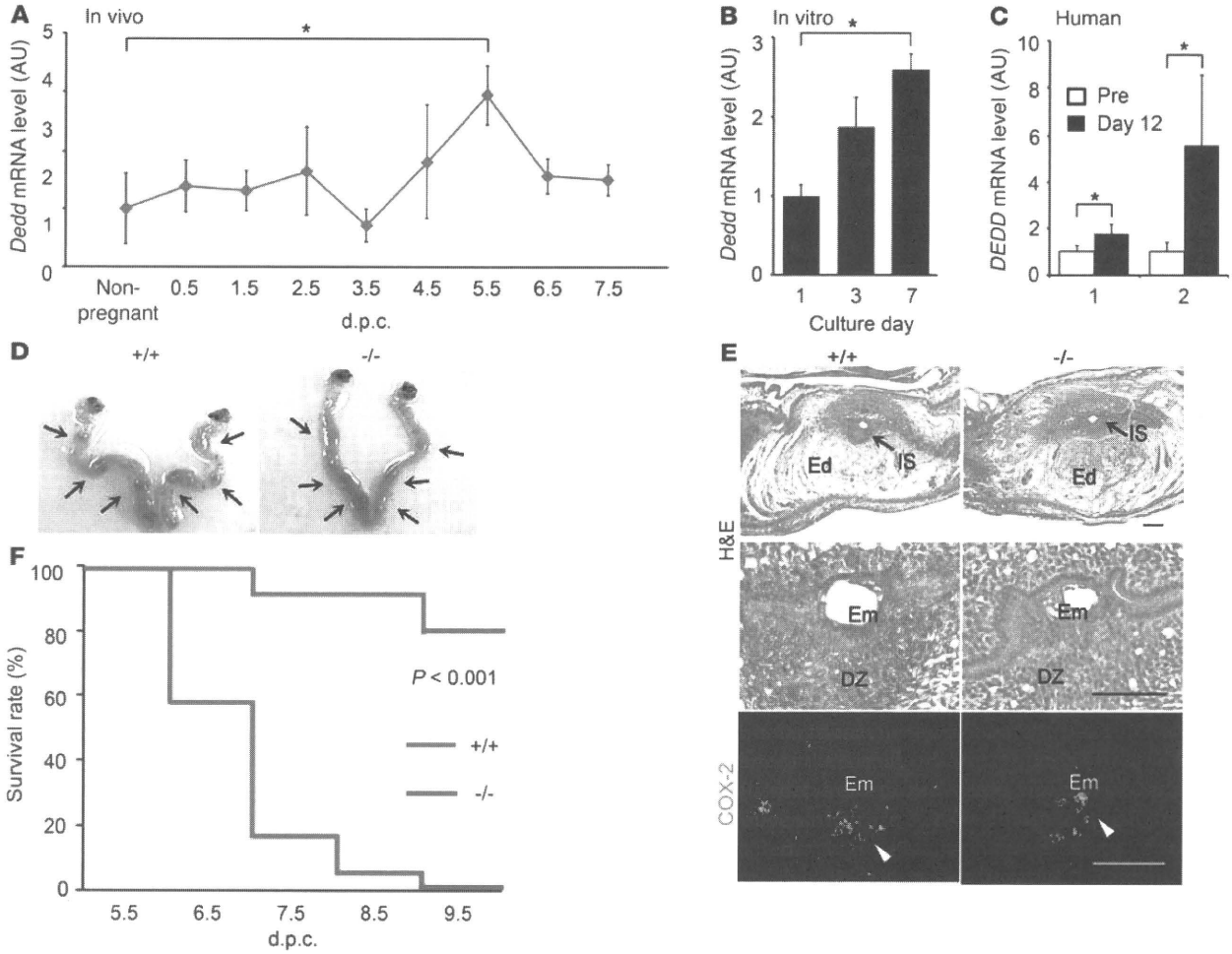

Figure 1

Postimplantation embryonic death in *Dedd*$^{-/-}$ uteri. (**A**–**C**) Increase in *Dedd* mRNA level in response to implantation in wild-type mouse (**A**) or in vitro decidualization in mouse uterine stromal (**B**) and human endometrial (**C**) cells, assessed by QPCR. Values were normalized to those of β-*actin* or *GAPDH* and are presented as relative expression to those of nonpregnant (**A**), day 1 (**B**), or undifferentiated (**C**) controls. Pre, undifferentiated cells; Day 12, decidualized cells at 12 days after the differentiation induction. In **C**, results from triplicate experiments using specimens from two individuals (1 and 2) are shown. Error bars indicate SEM. (**D**) Embryo spacing and crowding were assessed by blue dye injection. Representative photos of the uteri are shown. (**E**) Histologic analysis of implantation sites at 4.5 dpc in *Dedd*$^{+/+}$ (+/+) and *Dedd*$^{-/-}$ (–/–) uteri. Sections were stained with H&E or immunostained for COX-2. Em, embryo; DZ, decidual zone; Ed, edematous region (outside of DZ, white zone). Positive signals for COX-2 are indicated by arrowheads. Scale bars: 200 μm. (**F**) Survival rates of embryos during early gestation (Kaplan-Meier method). When embryo bodies were observed, regardless of size, they were regarded as "alive," whereas degenerated masses or those with scars at implantation sites were regarded as "dead." $n = 75$ for *Dedd*$^{+/+}$ and $n = 44$ for *Dedd*$^{-/-}$ uteri; log-rank, $\chi^2 = 13.2$. $^*P < 0.05$.

mice and $1.21 \times 10^6 \pm 0.075 \times 10^6$ in *Dedd*$^{+/+}$ mice; $n = 3$ each). Consistent with this result, when decidualizing stromal cells were challenged in vitro with 5-ethynil-2′-deoxyuridine (EdU; a nucleotide analog of thymidine), the proportion of EdU-incorporated cells was equivalent in *Dedd*$^{-/-}$ and *Dedd*$^{+/+}$ cells (Supplemental Figure 4A). Also, in vivo, 5.5-dpc implantation sites in *Dedd*$^{-/-}$ and *Dedd*$^{+/+}$ uteri stained similarly for Ki67, which identifies proliferating cells (Supplemental Figure 4B).

Decreased Akt level in Dedd$^{-/-}$ *uteri and increase in polyploidy by Akt expression in Dedd*$^{-/-}$ *decidual cells.* As we reported previously, the amount of Akt (all isotypes) is decreased in various *Dedd*$^{-/-}$ tissues, owing to decreased Akt protein stability (11). Notably, implantation sites in 5.5-dpc *Dedd*$^{-/-}$ uteri also showed decreased levels of Akt protein compared with those in *Dedd*$^{+/+}$ uteri, as assessed by immunoblotting with a pan-Akt antibody (Figure 4A). Parallel results were also obtained using in vitro decidualizing cells (Supplemental Figure 5). Signal for activated Akt phosphorylated at Thr308 was also decreased (Figure 4A, p-Akt). As we observed in mouse embryonic fibroblasts (MEFs) and other tissues (11), mRNA levels for *Akt1* and *Akt2* did not decrease in these cells (data not shown). To test whether the decrease in Akt protein was essential for the defect in polyploidy observed in *Dedd*$^{-/-}$ decidual cells (Figure 3), Akt-1 was overexpressed in in vitro differentiating *Dedd*$^{-/-}$ uterine stromal cells, and polyploidy was analyzed. As expected, the proportion of polynuclear cells was significantly increased by forced Akt-1 expression (Figure 4B). Thus, a decrease in Akt protein level appeared to be responsible for the inefficient decidualization observed in *Dedd*$^{-/-}$ uteri.

Table 2
Embryo size within *Dedd*$^{+/+}$ and *Dedd*$^{-/-}$ uteri

	Maternal genotype	Embryo size (mm^3)	*n*
Day 5.5	+/+	0.0059 ± 0.0014	9
	–/–	0.0039 ± 0.0012^A	9
Day 6.5	+/+	0.17 ± 0.014	5
	–/–	0.044 ± 0.0096^B	12
Day 7.5	+/+	0.51 ± 0.070	19
	–/–	0.25 ± 0.099^A	11
Day 8.5	+/+	>5.00	11
	–/–	1.00 ± 0.33	7

Both *Dedd*$^{+/+}$ (+/+) females and *Dedd*$^{-/-}$ (–/–) females were mated with *Dedd*$^{+/+}$ males. Therefore, embryos in *Dedd*$^{+/+}$ uteri were either *Dedd*$^{+/-}$ or *Dedd*$^{+/+}$, whereas those in *Dedd*$^{-/-}$ uteri were all *Dedd*$^{+/-}$. There was no significant difference in the size among the *Dedd*$^{+/-}$ and *Dedd*$^{+/+}$ embryos in *Dedd*$^{+/+}$ uteri. $^AP < 0.05$, $^BP < 0.001$.

Dedd associates with cyclin D3 and supports its protein stability. Of the multiple functions of Akt, control of the cell cycle via regulation of D-type cyclins in terms of gene expression, protein stability, and localization within the cell has been documented in different physiologic and pathologic situations (18). Das and colleagues recently implicated cyclin D3 as a key regulator of polynuclearization (7, 19, 20). In addition, García-Morales et al. showed that the protein stability of cyclin D3 is downregulated by rapamycin, an inhibitor of mammalian target of rapamycin (mTOR), downstream of Akt in the PI3K signaling pathway (21). This suggests that the decrease in Akt protein in the absence of DEDD might influence cyclin D3, resulting in a defect in polyploidy. To test this, we stained *Dedd*$^{-/-}$ and *Dedd*$^{+/+}$ uteri for cyclin D3 at 5.5 dpc. As shown in Figure 5A, *Dedd*$^{-/-}$ decidua harbored fewer cyclin D3–positive cells. This decrease in cyclin D3 was confirmed by immunoblotting (Figure 5B). However, the mRNA level for cyclin D3 was similar in *Dedd*$^{-/-}$ and *Dedd*$^{+/+}$ uteri at 5.5 d.p.c (Figure 5C), suggesting that the stability of cyclin D3 is affected in *Dedd*$^{-/-}$ cells. Therefore, we measured the half-life of cyclin D3 protein in in vitro differentiating stromal cells at day 3. Importantly, the amount of cyclin D3 protein started to decrease within 30 minutes in *Dedd*$^{-/-}$ cells but not in *Dedd*$^{+/+}$ cells (Figure 5D). By 90 minutes, the protein level of cyclin D3 was more than 3-fold lower in *Dedd*$^{-/-}$ compared with *Dedd*$^{+/+}$ cells (Figure 5D). The presence of MG132, a proteasome inhibitor, tempered the decrease observed in *Dedd*$^{-/-}$ cells (Figure 5D). Thus, lack of DEDD resulted in instability of cyclin D3. As in the case of Akt, increase in cyclin D3 protein by overexpression improved polyploidy in *Dedd*$^{-/-}$ decidual cells (Figure 5E), indicating that a decrease in cyclin D3 protein level also appeared to be involved in the inefficient decidualization observed in *Dedd*$^{-/-}$ uteri.

Such a relationship among DEDD, cyclin D3, and Akt was also supported by an in situ mRNA analysis using 5.5- and 7.5-dpc *Dedd*$^{+/+}$ uteri, which demonstrated coexpression of these 3 genes at the decidual zone cells in vivo (Figure 6A). Furthermore, DEDD associated with cyclin D3. This is similar to our previous observations that DEDD binds to various proteins such as cyclin B1, S6K1, and Akt (8–11). As shown in Figure 6B, immunoprecipitation in HEK293T cells expressing both FLAG-tagged cyclin D3 and hemagglutinin-tagged (HA-tagged) DEDD showed that the two proteins coprecipitated, indicating that DEDD may facilitate a complex with cyclin D3. Therefore, DEDD might support the stability of cyclin D3 by two independent pathways: maintenance of the Akt protein level and direct formation of a DEDD/cyclin D3 complex. HA-tagged DEDD also coprecipitated with FLAG-tagged Cdk4 and Cdk6 (Figure 6B). Endogenous DEDD was also coprecipitated with cyclin D3, Cdk4, or Cdk6, when tested using protein isolated from implantation sites of 5.5-dpc uteri (Figure 6C). Similar to our observation that DEDD associates with Cdk1/cyclin B1 via direct binding to cyclin B1, DEDD might form a complex with Cdk4/cyclin D3 and Cdk6/cyclin D3, both of which are essential for the regulation of decidualization (9), via a direct association with cyclin D3.

Discussion

A new role for DEDD in uterine decidualization and female fertility. Results of the present study implicate DEDD as an indispensable element in supporting early pregnancy. First, DEDD was expressed in decidual cells, and its absence decreased the Akt protein level in these cells. Second, the lack of DEDD decreased the stability of cyclin D3. Third, *Dedd*$^{-/-}$ stromal cells showed defective polyploidy during decidualization. Fourth, in *Dedd*$^{-/-}$ uteri, inefficient polyploidy disturbed development of the decidual zone, which was accompanied by disintegrated structure of the implantation site. As a result of these defects, *Dedd*$^{-/-}$ uteri cannot support embryonic growth before the development of the placenta, resulting in complete infertility of *Dedd*$^{-/-}$ female mice.

The decidual cell polyploidy, which is a hallmark of mature decidual cells particularly in mice, is characterized by the formation of large mono- or binucleated cells, consisting of DNA with multiples of the haploid complement (22–24). Although it has been suggested that various biological processes including metabolic activity are associated with the polyploidy (25), the physiological significance of this event in uterine decidualization remains poorly understood. Complete infertility in female *Dedd*$^{-/-}$ mice whose decidua showed a normal proliferative activity but less polyploidy may suggest the functional importance of polyploidy for the support of embryonic growth during early pregnancy.

It could be argued that the general effect of DEDD deficiency, such as decreased body size and mild attenuation of insulin production (8–11), might cause infertility. However, this is unlikely, given that female *S6K1*$^{-/-}$ mice, which show a similar (or even more advanced) phenotype regarding body size and insulin production, remain fertile (12). Similarly, although *Akt1*$^{-/-}$ mice also showed fetal growth impairment due to placental inefficiency, adult females are fertile (26).

Association of DEDD with decidual polyploidy via support of Akt and cyclin D3 stability. One reason why the absence of DEDD causes infertility appears to be the decrease in the amount of Akt protein in uterine stromal/decidual cells. Recent evidence in humans and mice suggests that Akt may play a role in the regulation of decidualization and in the survival of decidual cells. Of note, Hirota et al. showed increased decidual polyploidy with upregulation of Akt phosphorylation in mice with deficiency for p53 restricted to the uterus (27). As we reported previously, DEDD forms a complex with Akt and heat shock protein 90 (Hsp90) and stabilizes all isoforms of Akt protein (11). It is possible that defective protein stability of cyclin D3 may be brought about, in part, by a decrease in Akt, based on the facts that D-type cyclins are substrates for Akt, cyclin D3 is regarded as a major regulator of polyploidy, and the deficient polyploidy observed in *Dedd*$^{-/-}$ cells was improved by forced expression of Akt-1. Nevertheless, the precise machinery whereby Akt influences the stability of cyclin D3 is not yet clear.

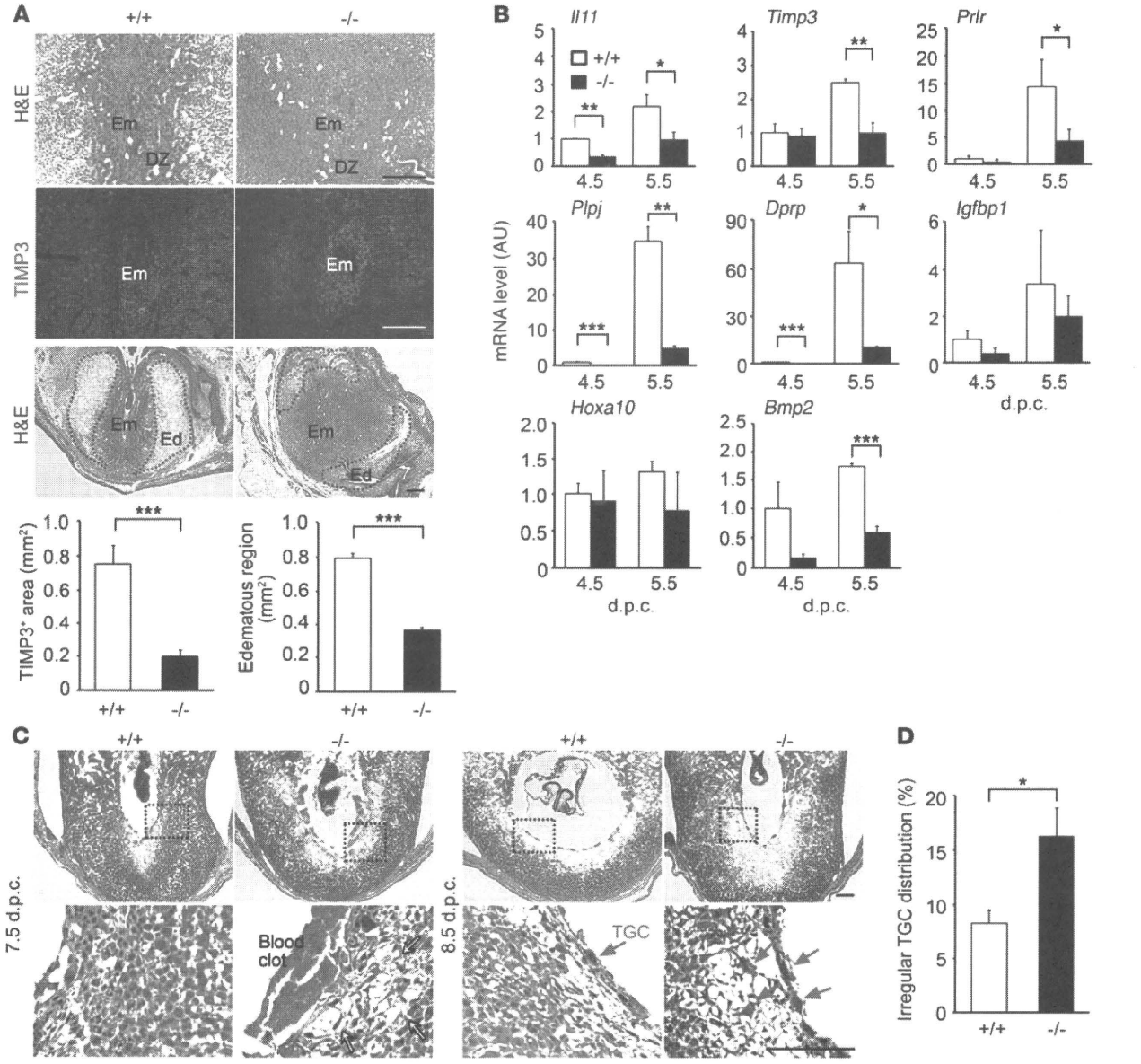

Figure 2

Defective decidualization in *Dedd*$^{-/-}$ uteri. (**A**) Implantation sites of 5.5-dpc *Dedd*$^{+/+}$ and *Dedd*$^{-/-}$ uteri were stained with H&E or immunostained for TIMP3. Scale bars: 200 μm. Quantification of decidual zone (TIMP3-positive area) and edematous region is also presented. At least 10 different sections in 3 different implantation sites were analyzed for each. Error bars indicate SEM. (**B**) mRNA levels of various genes that are highly expressed in decidua were analyzed by QPCR with total RNA isolated from 3 different implantation sites at 4.5 or 5.5 dpc. Values were normalized to those of β-*actin* and are presented as relative expression to 4.5-dpc *Dedd*$^{+/+}$ mice. Error bars indicate SEM. *Prlr*, prolactin receptor; *Plpj*, prolactin-like protein J; *Dprp*, decidual prolactin-related protein; *Igfbp1*, IGF-binding protein 1. (**C**) Histologic analysis of 7.5- and 8.5-dpc uteri (H&E staining). Higher magnification of the boxed area in the respective upper panel is presented in the lower panel. Arrows at 7.5 dpc indicate shrunken cells in *Dedd*$^{-/-}$ uterus. TGCs are denoted by blue arrows. Scale bars: 200 μm. (**D**) Irregular distribution of TGCs in *Dedd*$^{-/-}$ uterus. TGC numbers at the antimesometrial region of implantation sites were determined microscopically. At least 10 sections from 3 different specimens were examined. Data are shown as relative proportion of TGCs showing irregular distribution (invasion into the inner area). Error bars indicate SEM. $^{*}P < 0.05$, $^{**}P < 0.01$, $^{***}P < 0.001$.

Further studies are required to address the molecular mechanism. Interestingly, DEDD associates with cyclin D3; this might contribute structurally to the protein stability of cyclin D3.

Because cyclin D3–deficient mice do not show complete infertility, as observed in *Dedd*$^{-/-}$ mice (19, 28), a combination of various defects at the implantation site in addition to inefficient polyploidy — such as inadequate development of the edematous region (Figure 2A) and disintegrated structure of the implantation site at 7–8 d.p.c (Figure 2C) — might contribute to the overall infertility observed in *Dedd*$^{-/-}$ mice. These defects may also result from the decreased Akt level, given that Akt has diverse functions, including the maintenance of vascular permeability and an

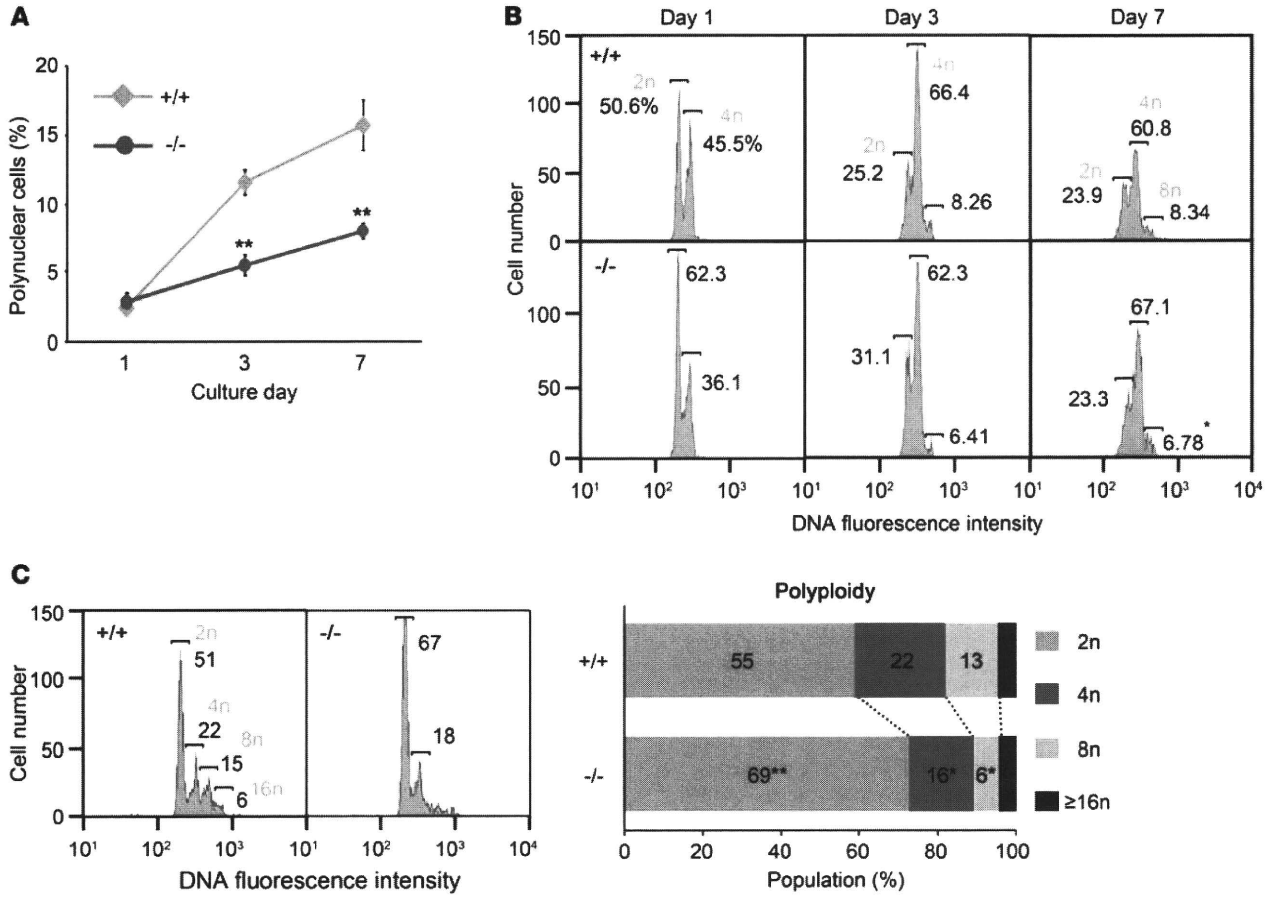

Figure 3

Attenuated polyploidy in *Dedd*$^{-/-}$ decidual cells. (**A**) In vitro decidualizing uterine stromal cells were stained with Hoechst to identify nuclei after different times in culture, and the number of polynuclear cells among 600 cells was counted microscopically. Analysis was performed by 3 independent researchers. (**B** and **C**) Quantification of DNA in in vitro decidualizing uterine stromal cells (**B**) or ex vivo stromal cells isolated from 4.5-dpc implantation sites (**C**). Cells were stained with Hoechst and analyzed by flow cytometry. Three independent experiments were performed, and a representative set of profiles is presented. In **C**, the average sizes for 2n, 4n, 8n, and ≥16n populations are also presented (right panel). $^{**}P < 0.01$.

antiapoptotic effect, in addition to regulation of the cell cycle (29–31). It is also noteworthy that no reproductive defects have been reported in mice deficient in Akt-1, -2, or -3, with the exception of two reports that *Akt1*$^{-/-}$ mice harbor a partial defect in follicular development within the ovary (32, 33). Thus, each Akt isoform may be functionally redundant in supporting fertility, given that *Dedd*$^{-/-}$ mice in which levels of all isoforms of Akt are decreased show a dramatic uterine defect (11). Our finding that the back-expression of Akt-1 efficiently recovered polyploidy in *Dedd*$^{-/-}$ stromal cells may support this idea. Unfortunately, mice doubly or triply deficient for multiple types of Akt die before they reach reproductive age (34). Future creation and analysis of conditional knockout mice in which various types of Akt are specifically deficient in the uterus will help to elucidate the involvement of Akt in fertility.

Perspectives. Our present findings identifying DEDD as an indispensable element in support of early pregnancy might shed light on the pathogenesis of infertility of unknown cause. Indeed, *DEDD* expression in uterine stromal cells increases along with decidualization both in mice and humans. In women experiencing implantation failure, one-third of the failures have been attributed to the embryo itself (35). Although the remaining two-thirds of failures appear to be the result of an inadequate uterine environment, the precise defect is often unknown. Thus, it may be worth addressing whether DEDD dysfunction is present in infertile women, either genetically or functionally, in uterine stromal cells. This may contribute to the development of new therapeutic strategies for infertility, though association of DEDD function with polyploidization as well as Akt and cyclin D3 in humans certainly needs to be further assessed.

Methods

Mice and human specimens. Dedd$^{-/-}$ mice had been cross-bred to C57BL/6 for 17 generations before being used for experiments. Female mice of 2–6 months of age were used. The day of the vaginal plug was considered as 0.5 dpc. Pseudopregnant mice were produced by mating female mice with vasectomized male mice of the CD-1 strain. All mice were maintained under specific pathogen-free conditions. All animals used in the experiments were cared for in accordance with institutional guidelines. Human endometrial tissue was obtained from women with benign diseases. The experimental procedures were approved by the institutional review board of the University of Tokyo, and all women provided written informed consent for the use of their endometrial tissue.

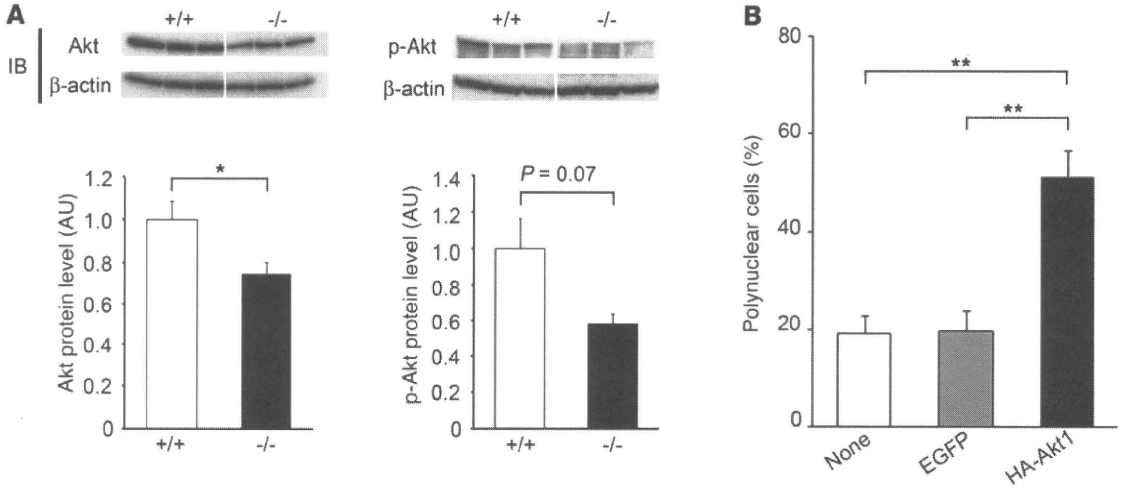

Figure 4
Involvement of Akt level in defective polyploidy in *Dedd*$^{-/-}$ decidual cells. (**A**) Immunoblotting of *Dedd*$^{+/+}$ and *Dedd*$^{-/-}$ uteri at 5.5 dpc for total Akt (left) and phosphorylated Akt (at Thr308, right). Three mice were analyzed. Quantification was performed with NIH Image J software. Values are presented as protein levels relative to those from *Dedd*$^{+/+}$ uteri. Error bars indicate SEM. (**B**) In vitro decidualizing *Dedd*$^{-/-}$ stromal cells were transfected with expression vector for HA-Akt1 or control EGFP at day 2. At day 5, cells were stained for HA and Hoechst; thereafter, the proportion of polynuclear cells among more than 100 HA-positive cells was evaluated microscopically. Average results from 4 independent sets of experiment are presented. Error bars indicate SEM. $^{*}P < 0.05$, $^{**}P < 0.01$.

Reagents and antibodies. Antibodies and reagents used were as follows. Primary antibodies were: ant-COX-2 (polyclonal, Cell Signaling Technology); anti-TIMP3 (W-18, Santa Cruz Biotechnology Inc.); anti-Akt (pan) (11E7, Cell Signaling Technology); anti-Ki67 (SP6, Thermo Scientific); anti-phospho-Akt (Thr308) (244F9, Cell Signaling Technology); anti-cyclin D3 (C-16, Santa Cruz Biotechnology Inc.) for immunohistochemistry; anti-cyclin D3 (DCS-22, Thermo Scientific) for immunoblotting and immunoprecipitation; anti-Cdk4 (DCS-35, Thermo Scientific); anti-Cdk6 (DCS-83, Thermo scientific); anti-β-actin (ACTN05 [C4], Abcam); anti-HA high-affinity antibody (3F10, Roche); and anti-FLAG antibody (M2, Sigma-Aldrich). Secondary antibodies and related reagents were: Alexa Fluor 488–conjugated anti-rabbit IgG antibody (Invitrogen); Alexa Fluor 546–conjugated anti-goat IgG antibody (Invitrogen); Hoechst 33258 and Hoechst 33324 (Invitrogen); Protein Block Serum-Free (Dako Cytomation); normal goat serum (Wako); Mayer's hematoxylin (Muto Pure Chemicals Co. Ltd.); eosin Y solution (Sigma-Aldrich); HRP-conjugated anti-mouse IgG (Pierce); and HRP-conjugated anti-rabbit IgG (Pierce).

Analysis of ovulation and fertilization. Briefly, superovulation was induced by intraperitoneal injection of pregnant mare serum gonadotropin (PMSG) (at -2.5 dpc; 5 IU/mouse) and human chorionic gonadotropin (hCG) (at -0.5 dpc; 5 IU/mouse). Oviducts from mated females were flushed with M2 medium at 0.5 dpc. Under a microscope, numbers of eggs were determined, and fertilization efficiency was evaluated by morphology of the eggs (i.e., having 2 nuclei or a fused large nucleus).

Histologic and immunohistochemical analysis. Uterine specimens were fixed by infusion of 4% PFA. For immunohistochemistry, deparaffinized sections were boiled in 10 mM sodium citrate buffer, pH 6.0, by microwave for 10 minutes. After blocking, sections were incubated with primary antibodies at 4°C for 16 hours, followed by secondary antibodies at room temperature for 1 hour. Samples were counterstained with Hoechst 33258. The areas of TIMP3-positive region and edematous region were measured by ImageJ software (NIH). Similarly, the embryonic area was measured. The size of each embryo was calculated as the sum of the embryonic area multiplied by its thickness (10 μm/section).

In situ hybridization. A 433-bp DNA fragment corresponding to the nucleotide positions 81–513 of mouse *Dedd* was subcloned into pGEMT-Easy vector (Promega) and was used for generation of sense or antisense RNA probes. A 431-bp DNA fragment corresponding to the nucleotide positions 1082–1512 of mouse *cyclin D3* and a 694-bp DNA fragment corresponding to the nucleotide positions 1851–2544 of mouse *Akt1* were similarly prepared. Paraffin-embedded uterine sections (6 μm) were hybridized with digoxigenin-labeled RNA probes at 60°C for 16 hours. The bound label was detected using NBT-BCIP, an alkaline phosphate color substrate. The sections were counterstained with Kernechtrot (Muto Pure Chemicals Co. Ltd.).

Primary culture of uterine stromal cells. The isolation and culture of mouse uterine stromal cells were performed as previously described (36). Briefly, uterine horns on day 3.5 of pseudopregnancy were cut and washed in HBSS (Invitrogen) without Ca^{2+}/Mg^{2+} and phenol red but containing 100 U/ml penicillin and 100 μg/ml streptomycin (Pen Strep; Invitrogen) and 2.5 μg/ml amphotericin B (Sigma-Aldrich). Tissues were digested in HBSS containing 6 mg/ml dispase (Invitrogen) and 25 mg/ml pancreatin (Sigma-Aldrich) and subsequently treated with 0.5 mg/ml collagenase (Sigma-Aldrich). The digested cells were passed through a 70-μm nylon filter to eliminate clumps of epithelial cells and were plated at 5×10^5 cells per 25 cm^2. For in vitro decidualization, the adherent cells were cultured in phenol red–free DMEM and Ham's F-12 nutrient mixture (DMEM/F-12, 1:1) (Invitrogen) with 1% charcoal-stripped FBS (Invitrogen) and antibiotics, 17β-estradiol (E2, 10 nM) (Sigma-Aldrich), P4 (1 μM) (Sigma-Aldrich), and HB-EGF (30 ng/ml) (Sigma-Aldrich). The induction of differentiation was continued for 7 days without changing medium. Isolation and differentiation of human endometrial stromal cells were performed as described previously (37). Cells were treated with phenol red–free DMEM/F-12 containing 5% charcoal-stripped FBS, antibiotics, E2 (10 ng/ml), and P4 (100 ng/ml) for 12 days. Media were replenished every 3 days.

Analysis of cell cycle and polyploidization. Cell cycle was analyzed using the Click-iT EdU kit (Invitrogen). Cultured uterine stromal cells were harvested at days 1, 3, and 7 after 10 μM EdU incorporation for 2 hours each. Trypsinized cells were fixed with 4% PFA and permeabilized with saponin. Incorporated EdU

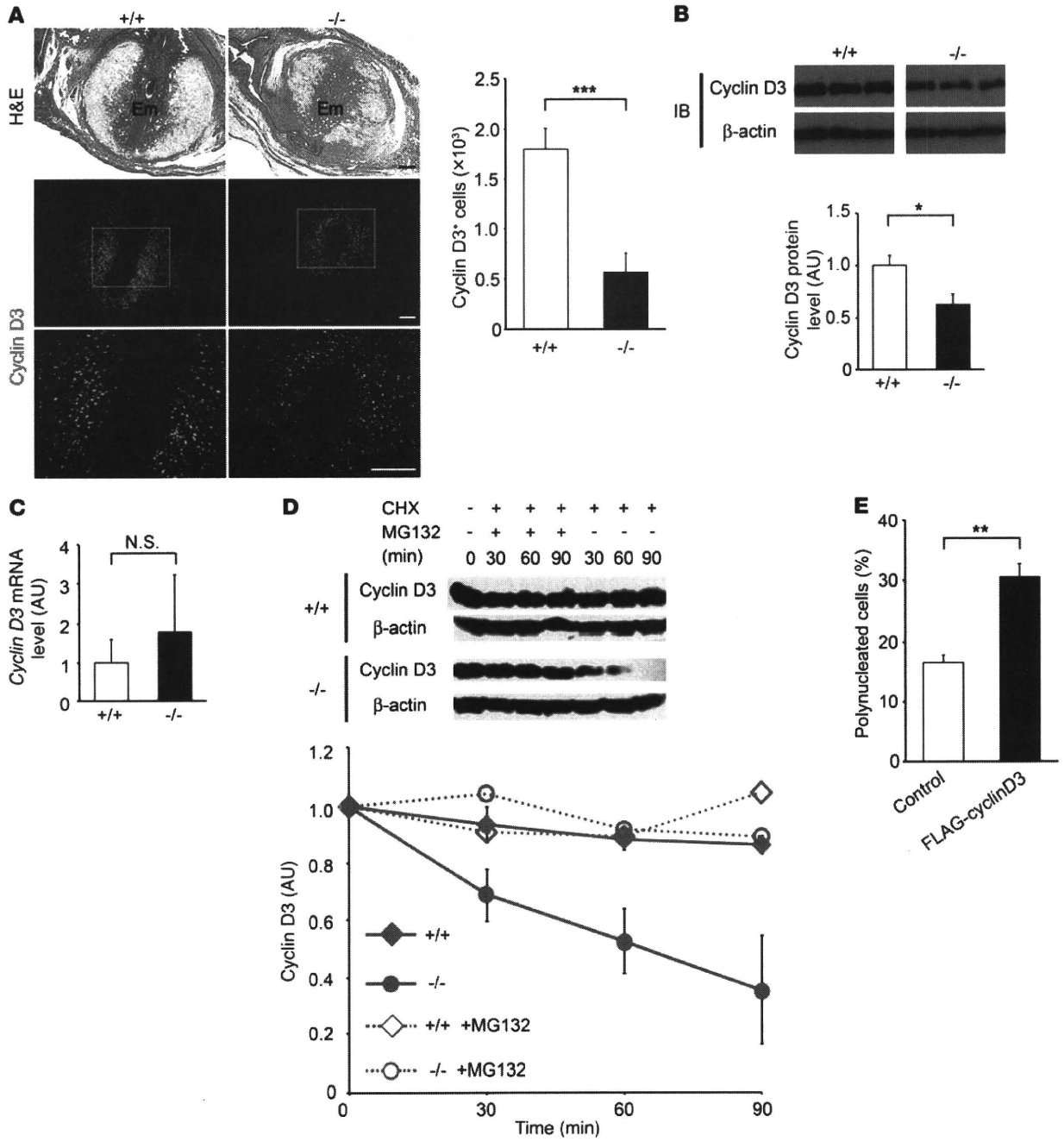

Figure 5

Decreased stability of cyclin D3 protein in *Dedd*$^{-/-}$ decidual cells. (**A**) At 5.5 dpc, implantation sites in *Dedd*$^{+/+}$ and *Dedd*$^{-/-}$ uteri were immunostained for cyclin D3. Bottom panels show higher magnifications of the dotted area in the middle panels. Scale bars: 200 μm. Graph on the right: Cyclin D3–positive cells within an implantation site were counted and compared in at least 4 different sections, and the means are presented. Error bars indicate SEM. (**B**) Immunoblotting of *Dedd*$^{+/+}$ and *Dedd*$^{-/-}$ uteri at 5.5 dpc for cyclin D3 and quantification of results. Three mice were analyzed. Error bars indicate SEM. (**C**) mRNA level for *cyclin D3* in 5.5-dpc implantation sites. No significant decrease in mRNA level was detected in *Dedd*$^{-/-}$ cells and tissues ($n = 3$ for each). (**D**) Protein degradation assay for cyclin D3. Uterine stromal cells at day 3 of in vitro decidualization were treated with cycloheximide (CHX; 50 μM) for the indicated periods in the presence or absence of proteasome inhibitor MG132 (10 μM). At each time point, cells were harvested, and the lysate was analyzed for cyclin D3 by immunoblotting. The amount of cyclin D3 protein at each time point was normalized to that of β-actin and is presented as relative level to that at pretreatment (0 minutes) in *Dedd*$^{+/+}$ or *Dedd*$^{-/-}$ cells. Three independent experiments were performed, and representative blots are presented. Error bars indicate SEM. (**E**) In vitro decidualizing *Dedd*$^{-/-}$ stromal cells were transfected with expression vector for FLAG–cyclin D3 at day 2. At day 5, cells were stained for FLAG and Hoechst; thereafter, the proportion of polynuclear cells among more than 100 FLAG-positive cells was evaluated microscopically. Average results from 4 independent sets of experiment are presented. Error bar indicate SEM. $^{*}P < 0.05$, $^{**}P < 0.01$, $^{***}P < 0.001$.

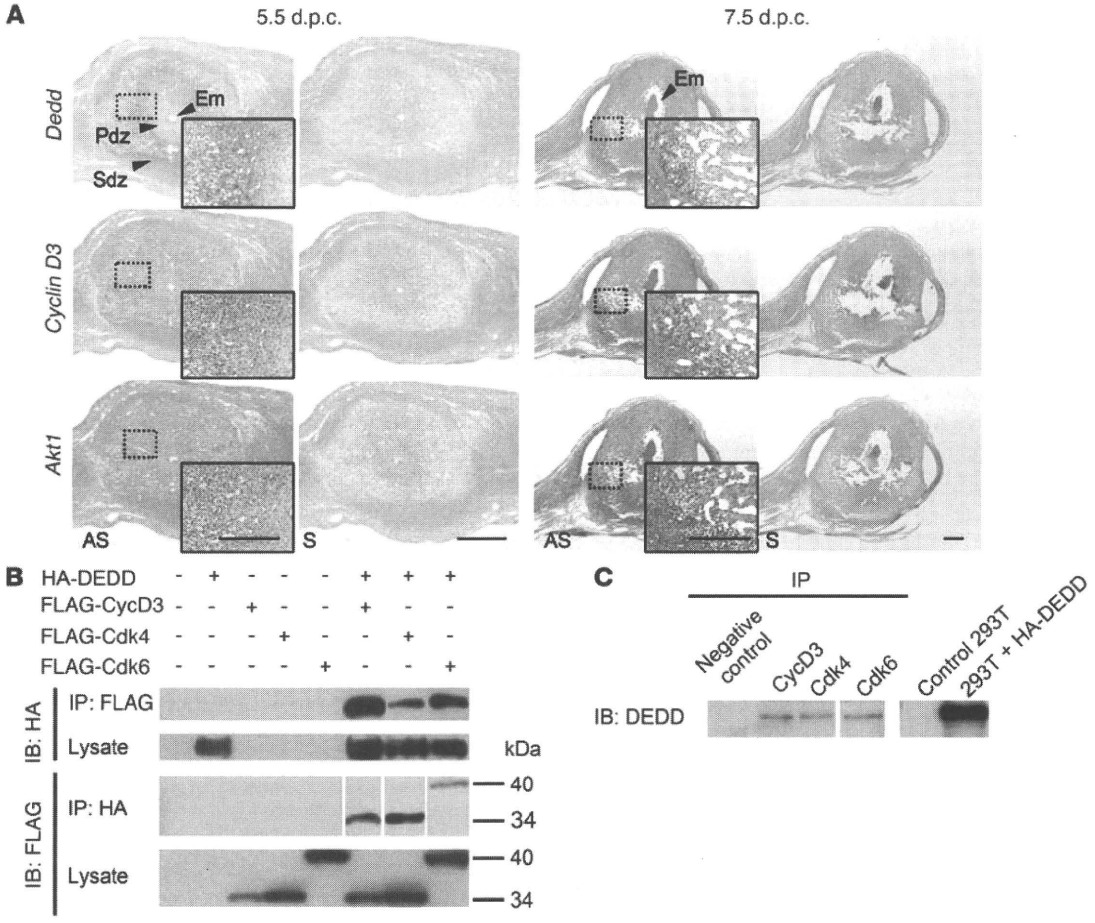

Figure 6

The association of DEDD with cyclin D3. (**A**) In situ mRNA analysis for *Dedd*, *cyclin D3*, and *Akt1* in 5.5- and 7.5- dpc wild-type mouse uteri. Microphotographs at a higher magnification are also presented. AS, antisense probe; S, sense control probe; Pdz, primary decidual zone; Sdz, secondary decidual zone. Scale bars: 500 μm. (**B**) Binding study. HA-tagged DEDD and FLAG-tagged cyclin D3, Cdk4, or Cdk6 were expressed in HEK293T cells, and association of HA-DEDD and each FLAG-tagged protein was evaluated by a coimmunoprecipitation assay with anti-HA or anti-FLAG antibody. (**C**) Coprecipitation of endogenous DEDD with cyclin D3, Cdk4, or Cdk6 from lysates of 5.5-dpc uterine implantation sites. Precipitates were immunoblotted with an anti-DEDD antibody. HEK293T cells with or without transfection of HA-tagged DEDD were used as controls.

was detected by an alkylation reagent conjugated with Alexa Fluor 488. DNA content was quantitatively detected by subsequent staining with Hoechst 33342. At least 10,000 cells for each sample were analyzed by flow cytometry. For evaluation of polyploidy, cells were cultured in a 4-well chamber and stained with Hoechst after fixation with 4% PFA. Multinucleated cells were calculated under a fluorescence microscope and counted by 3 independent researchers in a blinded fashion from more than 600 total cells each.

Flow cytometry (analysis of cell DNA contents). In vitro decidualizing cells were stained with Hoechst 33342 and analyzed for DNA content by an LSR II flow cytometer (BD). At least 10,000 cells were analyzed for each. For ex vivo cells, 4.5-dpc uterine implantation sites were digested by a collagenase treatment, and purified single cells were stained with Hoechst 33342. The large stromal cell population was gated, and at least 1,000 cells were analyzed for DNA content.

Akt and cyclin D3 overexpression in decidual cells. Uterine stromal cells at day 2 of culture in the presence of E2, P4, and HB-EGF were transfected with a pCruz-HA-Akt1, pFLAG-cyclinD3, or a mock expression vector by using Lipofectamine 2000 (Invitrogen). At day 5, cells were fixed with 4% PFA and permeabilized with 0.25% Triton X-100. The transfected cells were detected by anti-HA high-affinity antibody or anti-FLAG antibody conjugated with Cy3. Multinucleated cells were counted under a fluorescence microscope after Hoechst staining.

Protein degradation assay. Day 3 in vitro decidualizing stromal cells were treated with 50 μM cycloheximide (Sigma-Aldrich) in the presence or absence of 10 μM MG132 (Sigma-Aldrich) and were harvested at the indicated time points. Cells were lysed in a lysis buffer (1% NP-40, 150 mM NaCl, 50 mM Tris-HCl pH 7.4, 1 mM sodium orthovanadate, 1 mM sodium fluoride, and Complete Mini [Roche]) and used for immunoblotting.

Coimmunoprecipitation assay. HEK293T cells were transfected with pCAG-DEDD-HA, pFLAG-cyclin D3, pFLAG-Cdk4, or pFLAG-Cdk6 by electroporation. Cells were lysed and incubated with anti-HA or anti-FLAG beads for 16 hours at 4°C. Precipitates were analyzed for the presence of coprecipitated molecule by immunoblotting using anti-FLAG or anti-HA antibody. For the binding of endogenous DEDD with cyclin D3, Cdk4, or Cdk6, 5.5-dpc uterine implantation sites were homogenized in lysis buffer and incubated with anti-cyclin D3, anti-Cdk4, or anti-Cdk6 antibody bound to protein G beads. Precipitates were immunoblotted with an anti-DEDD polyclonal antibody prepared in-house (8).

Quantitative and semiquantitative RT-PCR. QPCR was performed using Power SYBR Green PCR Master Mix (Applied Biosystems) and the ABI Prism 7000 Sequence Detection System (Applied Biosystems). Results were analyzed by the ΔΔCt method, in which the Cts of β-actin were used for normalization. Primer sequences are detailed in Supplemental Table 1. For semiquantitative PCR shown in Supplemental Figure 3, primers are shown in Supplemental Table 2.

Statistics. All statistical analyses were performed using 2-tailed Student's *t* test. Standard deviation and variance of every data set were calculated, and the homoscedasticity was confirmed by *F* test. *P* values less than 0.05 were considered significant.

Acknowledgments

We thank to A. Kodama, T. Fujii, Y. Taketani, H. Kurihara, and Y. Kurihara (Tokyo), M. Noguchi (Sapporo), and A. Nishijima, for technical assistance and constructive discussion; Genostaff Co. Ltd. for in situ mRNA hybridization; and M. Miyamoto for administrative assistance. This work was supported by the Global COE Research Program, Uehara Memorial Foundation (to T. Miyazaki), and the Kanzawa Research Medical Foundation (to S. Arai).

Received for publication August 12, 2010, and accepted in revised form October 20, 2010.

Address correspondence to: Toru Miyazaki, Laboratory of Molecular Biomedicine for Pathogenesis, Center for Disease Biology and Integrative Medicine, Faculty of Medicine, The University of Tokyo, 7-3-1 Hongo, Bunkyo-ku, Tokyo 113-0033, Japan. Phone: 81.3.5841.1435; Fax: 81.3.5841.1438; E-mail: tm@m.u-tokyo.ac.jp.

Miwako Kitazume's present address is: Division of Developmental Genetics, National Institute of Genetics, Mishima, Shizuoka, Japan.

1. Wang H, Dey SK. Roadmap to embryo implantation: clues from mouse models. *Nat Rev Genet.* 2006;7(3):185–199.
2. Dey SK, et al. Molecular cues to implantation. *Endocr Rev.* 2004;25(3):341–373.
3. Das SK. Cell cycle regulatory control for uterine stromal cell decidualization in implantation. *Reproduction.* 2009;137(6):889–899.
4. Satokata I, Benson G, Maas R. Sexually dimorphic sterility phenotypes in Hoxa10-deficient mice. *Nature.* 1995;374(6521):460–463.
5. Lim H, Ma L, Ma WG, Maas RL, Dey SK. Hoxa-10 regulates uterine stromal cell responsiveness to progesterone during implantation and decidualization in the mouse. *Mol Endocrinol.* 1999;13(6):1005–1017.
6. Robb L, Li R, Hartley L, Nandurkar HH, Koentgen F, Begley CG. Infertility in female mice lacking the receptor for interleukin 11 is due to a defective uterine response to implantation. *Nat Med.* 1998;4(3):303–308.
7. Tan J, Raja S, Davis MK, Tawfik O, Dey SK, Das SK. Evidence for coordinated interaction of cyclin D3 with p21 and cdk6 in directing the development of uterine stromal cell decidualization and polyploidy during implantation. *Mech Dev.* 2002; 111(1–2):99–113.
8. Arai S, et al. Death-effector domain-containing protein DEDD is an inhibitor of mitotic Cdk1/cyclin B1. *Proc Natl Acad Sci U S A.* 2007;104(7):2289–2294.
9. Miyazaki T, Arai S. Two distinct controls of mitotic cdk1/cyclin B1 activity requisite for cell growth prior to cell division. *Cell Cycle.* 2007;6(12):1419–1425.
10. Kurabe N, et al. The death effector domain-containing DEDD supports S6K1 activity via preventing Cdk1-dependent inhibitory phosphorylation. *J Biol Chem.* 2009;284(8):5050–5055.
11. Kurabe N, et al. The death effector domain-containing DEDD forms a complex with Akt and Hsp90, and supports their stability. *Biochem Biophys Res Commun.* 2010;391(4):1708–1713.
12. Pende M, et al. Hypoinsulinaemia, glucose intolerance and diminished beta-cell size in S6K1-deficient mice. *Nature.* 2000;408(6815):994–997.
13. Paria BC, Huet-Hudson YM, Dey SK. Blastocyst's state of activity determines the "window" of implantation in the mouse receptive uterus. *Proc Natl Acad Sci U S A.* 1993;90(21):10159–10162.
14. Lim H, et al. Multiple female reproductive failures in cyclooxygenase 2-deficient mice. *Cell.* 1997;91(2):197–208.
15. Bany BM, Schultz GA. Tissue inhibitor of matrix metalloproteinase-3 expression in the mouse uterus during implantation and artificially induced decidualization. *Mol Reprod Dev.* 2001;59(2):159–167.
16. Hassan MQ, et al. HOXA10 controls osteoblastogenesis by directly activating bone regulatory and phenotypic genes. *Mol Cell Biol.* 2007;27(9):3337–3352.
17. Lee KY, et al. Bmp2 is critical for the murine uterine decidual response. *Mol Cell Biol.* 2007; 27(15):5468–5478.
18. Diehl JA, Cheng M, Roussel MF, Sherr CJ. Glycogen synthase kinase-3beta regulates cyclin D1 proteolysis and subcellular localization. *Genes Dev.* 1998;12(22):3499–3511.
19. Das SK. Regional development of uterine decidualization: molecular signaling by Hoxa-10. *Mol Reprod Dev.* 2010;77(5):387–396.
20. Das SK, Lim H, Paria BC, Dey SK. Cyclin D3 in the mouse uterus is associated with the decidualization process during early pregnancy. *J Mol Endocrinol.* 1999;22(1):91–101.
21. García-Morales P, Hernando E, Carrasco-García E, Menéndez-Gutierrez MP, Saceda M, Martínez-Lacaci I. Cyclin D3 is down-regulated by rapamycin in HER-2-overexpressing breast cancer cells. *Mol Cancer Ther.* 2006;5(9):2172–2181.
22. Sachs L, Shelesnyak MC. The development and suppression of polyploidy in the developing and suppressed deciduoma in the rat. *J Endocrinol.* 1955; 12(2):146–151.
23. Ansell JD, Barlow PW, McLaren A. Binucleate and polyploid cells in the decidua of the mouse. *J Embryol Exp Morphol.* 1974;31(1):223–227.
24. Moulton BC. Effect of progesterone on DNA, RNA and protein synthesis of deciduoma cell fractions separated by velocity sedimentation. *Biol Reprod.* 1979;21(3):667–672.
25. Edgar BA, Orr-Weaver TL. Endoreplication cell cycles: more for less. *Cell.* 2001;105(3):297–306.
26. Yang ZZ, et al. Protein kinase B alpha/Akt1 regulates placental development and fetal growth. *J Biol Chem.* 2003;278(34):32124–32131.
27. Hirota Y, Daikoku T, Tranguch S, Xie H, Bradshaw HB, Dey SK. Uterine-specific p53 deficiency confers premature uterine senescence and promotes preterm birth in mice. *J Clin Invest.* 2010;120(3):803–815.
28. Sicinska E, et al. Requirement for cyclin D3 in lymphocyte development and T cell leukemias. *Cancer Cell.* 2003;4(6):451–461.
29. Franke TF, Kaplan DR, Cantley LC. PI3K: downstream AKTion blocks apoptosis. *Cell.* 1997;88(4):435–437.
30. Burgering BM, Coffer PJ. Protein kinase B (c-Akt) in phosphatidylinositol-3-OH kinase signal transduction. *Nature.* 1995;376(6541):599–602.
31. Franke TF. Intracellular signaling by Akt: bound to be specific. *Sci Signal.* 2008;1(24):pe29.
32. Brown C, et al. Subfertility caused by altered follicular development and oocyte growth in female mice lacking PKBalpha/Akt. *Biol Reprod.* 2010;82(2):246–256.
33. Easton RM, et al. Role for Akt3/protein kinase Bgamma in attainment of normal brain size. *Mol Cell Biol.* 2005;25(5):1869–1878.
34. Peng XD, et al. Dwarfism, impaired skin development, skeletal muscle atrophy, delayed bone development, and impeded adipogenesis in mice lacking Akt1 and Akt2. *Genes Dev.* 2003;17(11):1352–1365.
35. Simón C, Moreno C, Remohí J, Pellicer A. Cytokines and embryo implantation. *J Reprod Immunol.* 1998;39(1–2):117–131.
36. Tan Y, et al. HB-EGF directs stromal cell polyploidy and decidualization via cyclin D3 during implantation. *Dev Biol.* 2004;265(1):181–195.
37. Kodama A, et al. Progesterone decreases bone morphogenetic protein (BMP) 7 expression and BMP7 inhibits decidualization and proliferation in endometrial stromal cells. *Human Reprod.* 2010;25(3):751–756.